

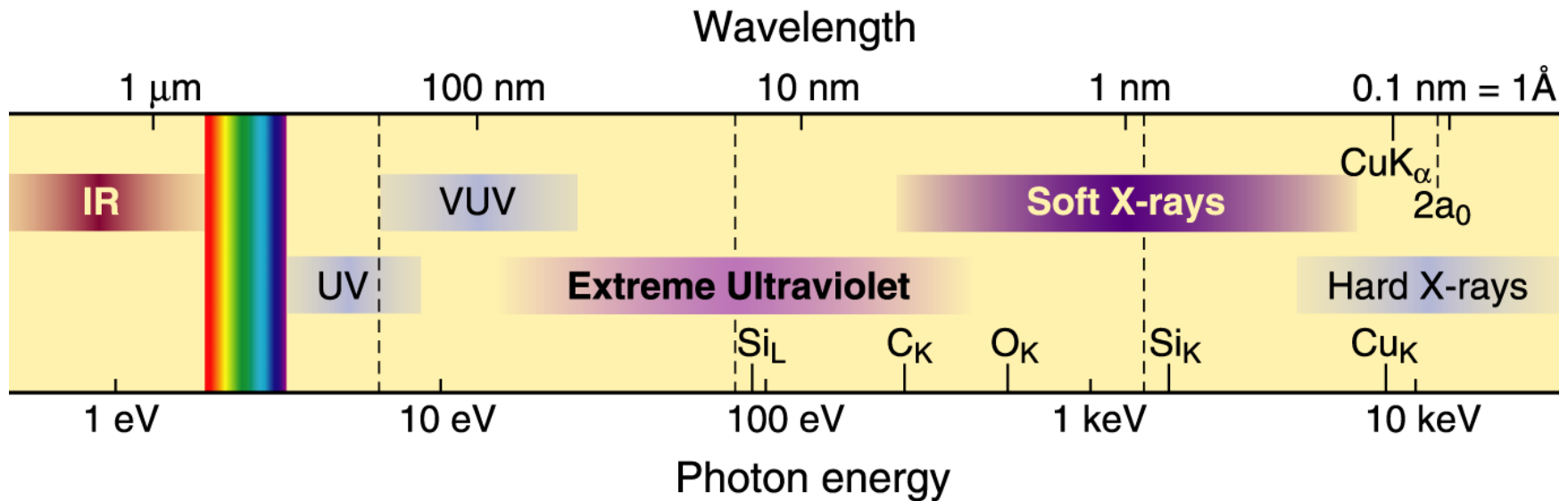


# Soft and Hard X-Ray Microscopy

David Attwood  
University of California, Berkeley

Cheiron School  
September 2013  
SPring-8

# The short wavelength region of the electromagnetic spectrum



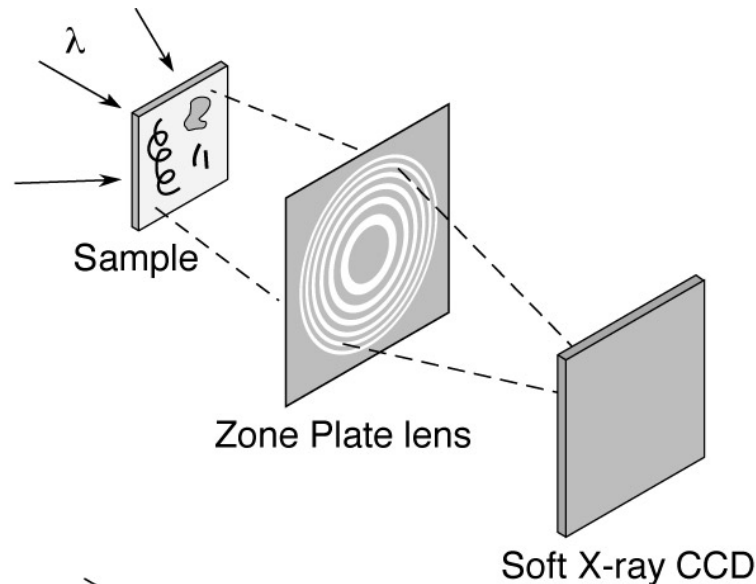
- See smaller features
- Write smaller patterns
- Elemental and chemical sensitivity

$$\hbar\omega \cdot \lambda = hc = 1239.842 \text{ eV nm}$$

$$n = 1 - \delta + i\beta \quad \delta, \beta \ll 1$$

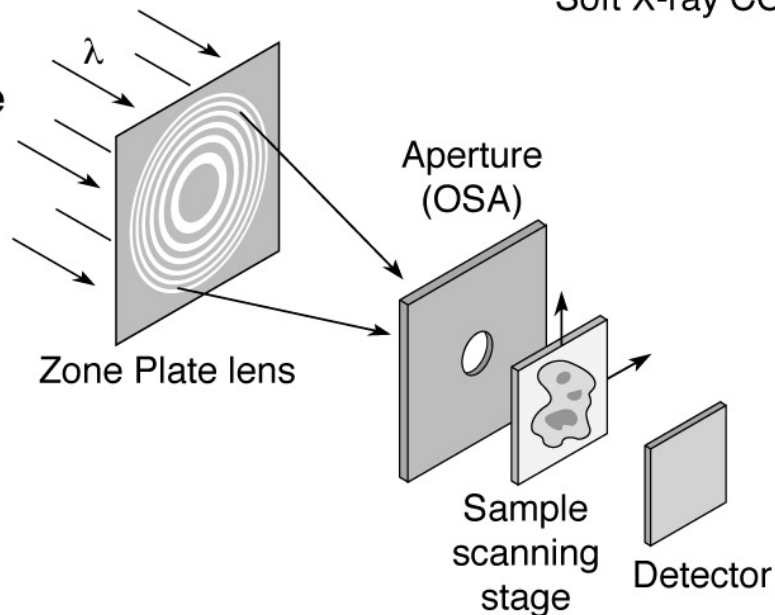
# Two common soft x-ray microscopes

## Full-Field Microscope



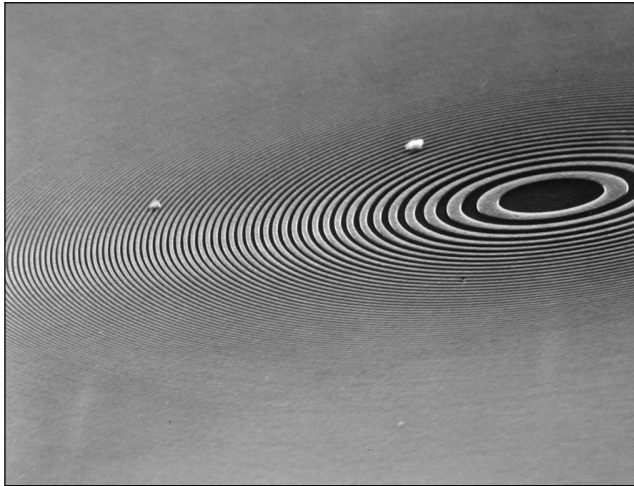
- 10–20 nm spatial resolution
- Modest spectral resolution
- Seconds exposure time
- Bending magnet radiation
- Higher radiation dose
- Flexible sample environment (wet, cryo, labeled magnetic fields, electric fields, cement, ...)

## Scanning Microscope

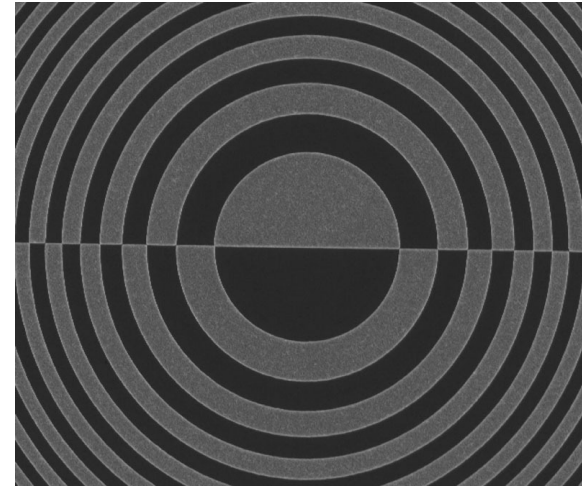


- 10–20 nm spatial resolution
- Least radiation dose
- Best spectral resolution
- Requires spatially coherent radiation
- Minutes exposure time
- Flexible sample environment
- Photoemission, fluorescence imaging

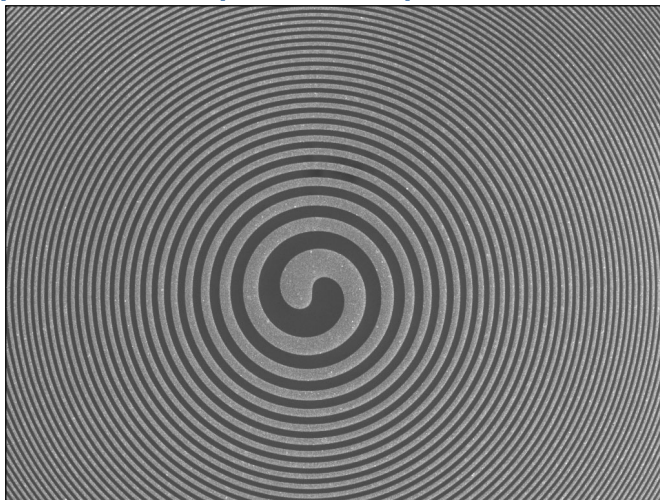
Soft x-ray zone plate



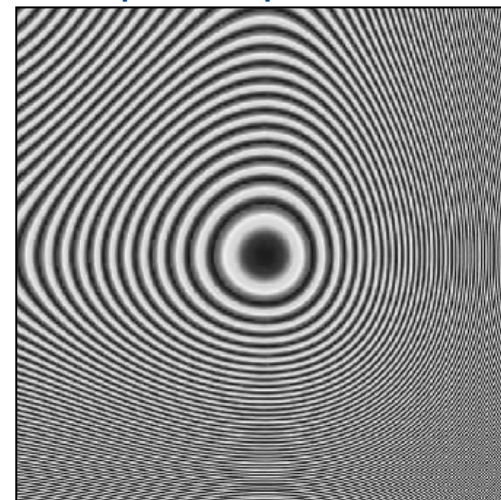
DIC microscopy



Spiral zone plate for phase contrast



Cubic phase plate for DOF



*Courtesy of Anne Sakdinawat, Chang Chang, Weilun Chao and Erik Anderson (LBNL & UCB.)*



### Soft X-ray microscopy at a spatial resolution better than 15 nm

Weilun Chao<sup>1,2</sup>, Bruce D. Harteneck<sup>1</sup>, J. Alexander Liddle<sup>1</sup>, Erik H. Anderson<sup>1</sup> & David T. Attwood<sup>1,2</sup>

Analytical tools that have spatial resolution at the nanometre scale are indispensable for the life and physical sciences. It is desirable that these tools also permit elemental and chemical identification on a scale of 10 nm or less, with large penetration depths. A variety of techniques<sup>1–7</sup> in X-ray imaging are currently being developed that may provide these combined capabilities. Here we report the achievement of sub-15-nm spatial resolution with a soft X-ray microscope—and a clear path to below 10 nm—using an overlay technique for zone plate fabrication. The microscope covers a spectral range from a photon energy of 250 eV (~5 nm wavelength) to 1.8 keV (~0.7 nm), so that primary K and L atomic resonances of elements such as C, N, O, Al, Ti, Fe, Co and Ni can be probed. This X-ray microscopy technique is therefore suitable for a wide range of studies: biological imaging in the water window<sup>8,9</sup>; studies of wet environmental samples<sup>10,11</sup>; studies of magnetic nanostructures with both elemental and spin-orbit sensitivity<sup>12–14</sup>; studies that require viewing through thin windows, coatings or substrates (such as buried electronic devices in a silicon chip<sup>15</sup>); and three-dimensional imaging of cryogenically fixed biological cells<sup>9,16</sup>.

The microscope XM-1 at the Advanced Light Source (ALS) in Berkeley<sup>17</sup> is schematically shown in Fig. 1. The microscope type is similar to that pioneered by the Göttingen/BESSY group (ref. 18, and references therein). A 'micro' zone plate (MZP) projects a full-field image to an X-ray-sensitive CCD (charge-coupled device), typically in one or a few seconds, often with several hundred images per day. The field of view is typically 10  $\mu\text{m}$ , corresponding to a magnification of 2,500. The condenser zone plate (CZP), with a central stop, serves two purposes in that it provides partially coherent hollow-cone illumination<sup>2</sup>, and, in combination with a pinhole, serves as the

monochromator. Monochromatic radiation of  $\lambda/\Delta\lambda = 500$  is used. Both zone plates are fabricated in-house, using electron beam lithography<sup>19</sup>.

The spatial resolution of a zone plate based microscope is equal to  $k_1\lambda/NA_{MZP}$ , where  $\lambda$  is the wavelength,  $NA_{MZP}$  is the numerical aperture of the MZP, and  $k_1$  is an illumination dependent constant, which ranges from 0.3 to 0.61. For a zone plate lens used at high magnification,  $NA_{MZP} = \lambda/2\Delta r_{MZP}$ , where  $\Delta r_{MZP}$  is the outermost (smallest) zone width of the MZP<sup>20</sup>. For the partially coherent illumination<sup>21,22</sup> used here,  $k_1 \approx 0.4$  and thus the theoretical resolution is  $0.8\Delta r_{MZP}$ , as calculated using the SPLAT computer program<sup>23</sup> (a two-dimensional scalar diffraction code, which evaluates partially coherent imaging). In previous results with a  $\Delta r_{MZP} = 25$  nm zone plate, we reported<sup>2</sup> an unambiguous spatial resolution of 20 nm. Here we describe the use of an overlay nanofabrication technique that allows us to fabricate zone plates with finer outer zone widths, to  $\Delta r_{MZP} = 15$  nm, and to achieve a spatial resolution of below 15 nm, with clear potential for further extension.

This technique overcomes nanofabrication limits due to electron beam broadening in high feature density patterning. Beam broadening results from electron scattering within the recording medium (resist), leading to a loss of image contrast and thus resolvability for

$$\lambda = 1.52 \text{ nm (815 eV)}$$

$$\Delta r = 15 \text{ nm}$$

$$N = 500$$

$$D = 30 \mu\text{m}$$

$$f = 300 \mu\text{m}$$

$$\sigma = 0.38$$

$$0.8 \Delta r = 12 \text{ nm}$$

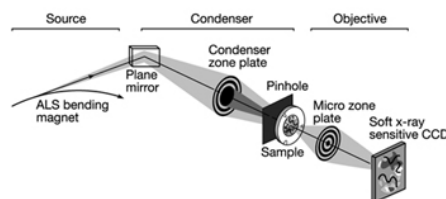


**Figure 1 | A diagram of the soft X-ray microscope XM-1.** The microscope uses a micro zone plate to project a full field image onto a CCD camera that is sensitive to soft X-rays. Partially coherent, hollow-cone illumination of the sample is provided by a condenser zone plate. A central stop and a pinhole provide monochromatization.

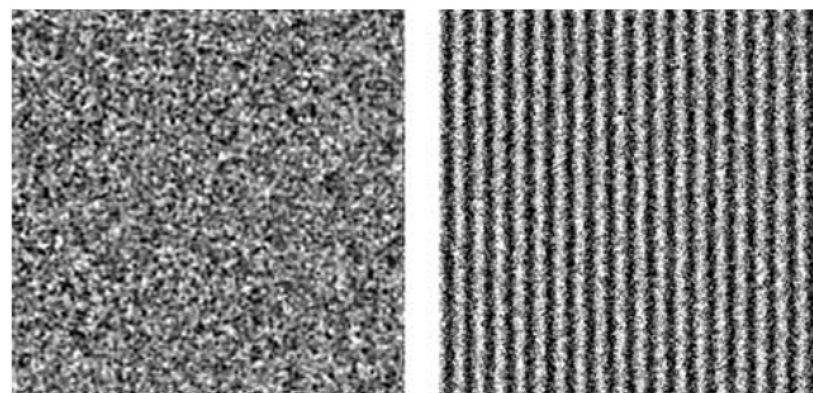
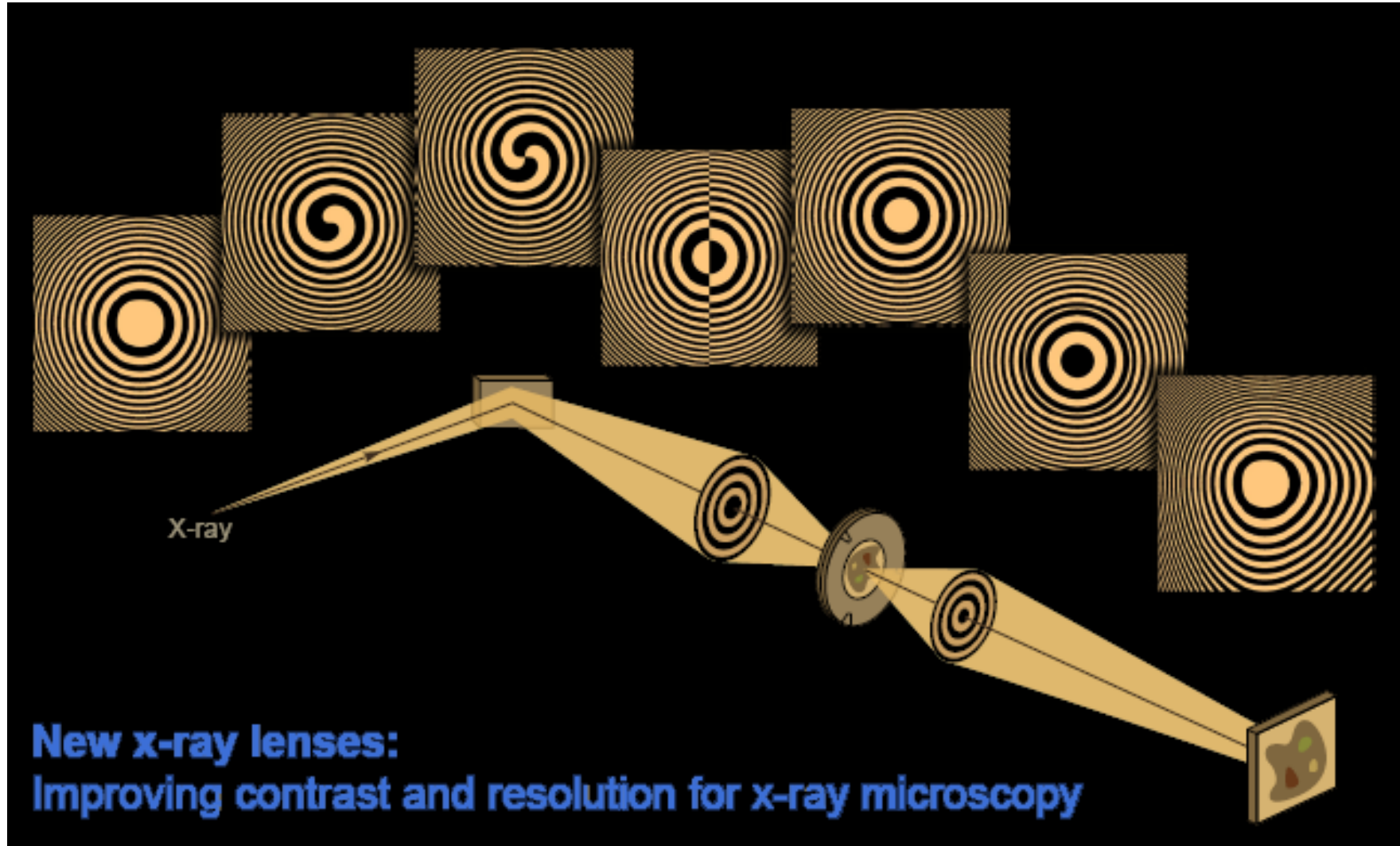


**Figure 4 | Soft X-ray images of a 15.1 nm half-period test object, as formed with zone plates having outer zone widths of 25 nm and 15 nm.**

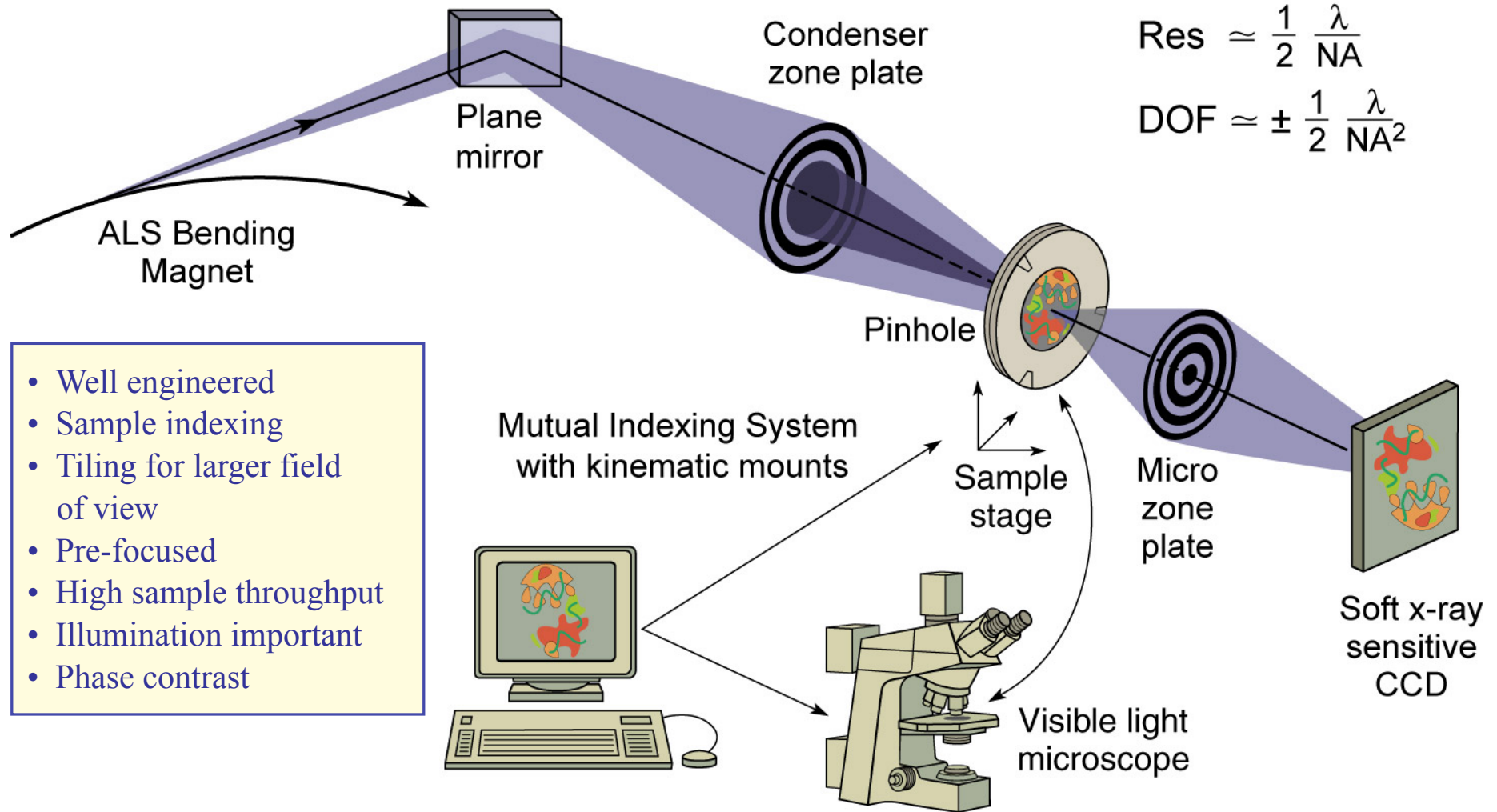
Cr/Si test pattern (Cr L<sub>3</sub> @ 574 eV)  
(2000 X 2000, 10<sup>4</sup> ph/pixel)

# Novel zone plates for specific functionality



Courtesy of Anne Sakdinawat, UC Berkeley

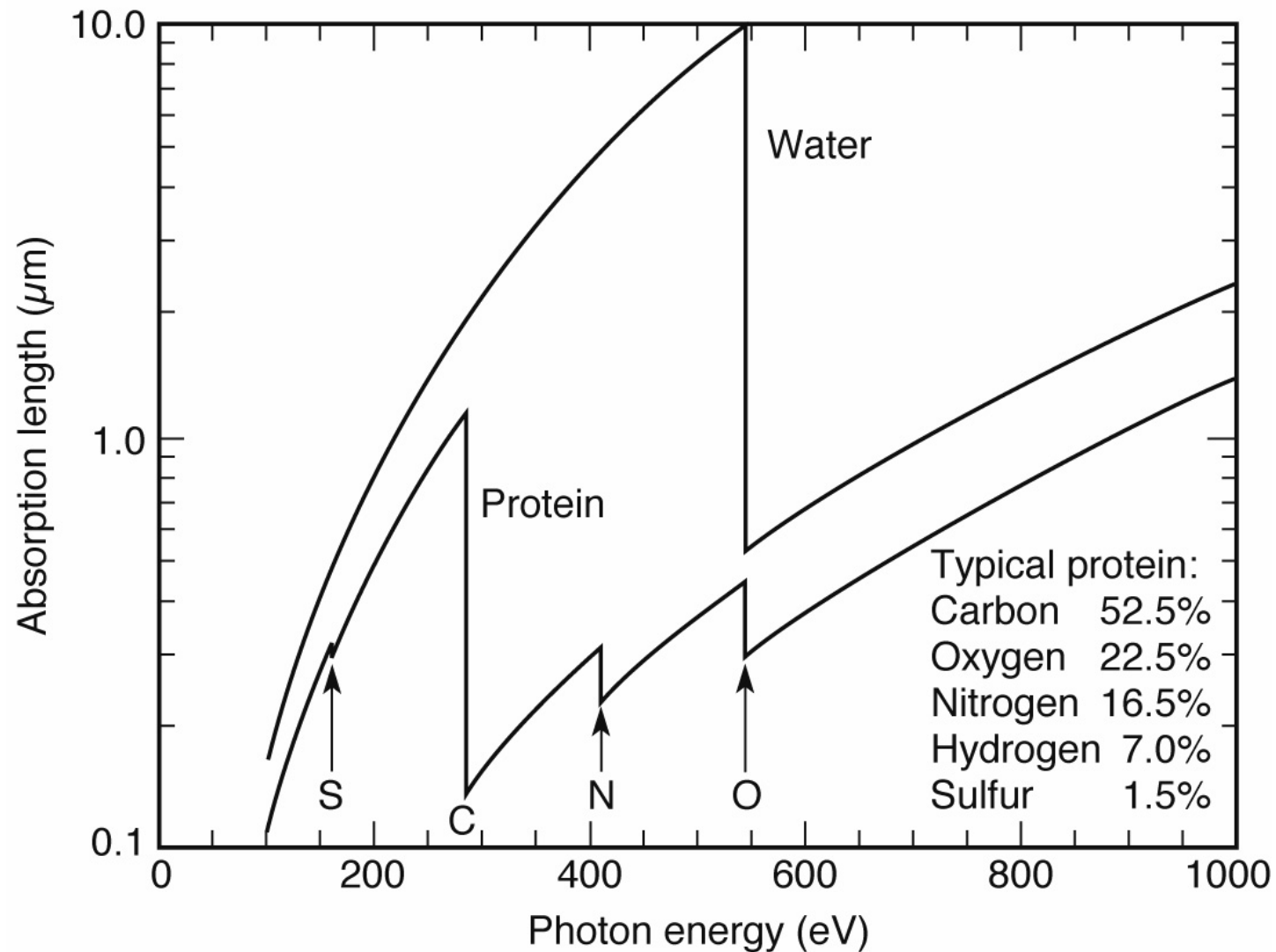
# High resolution zone plate microscopy



HiResZPMicrXM1Biology\_Jan08.ai

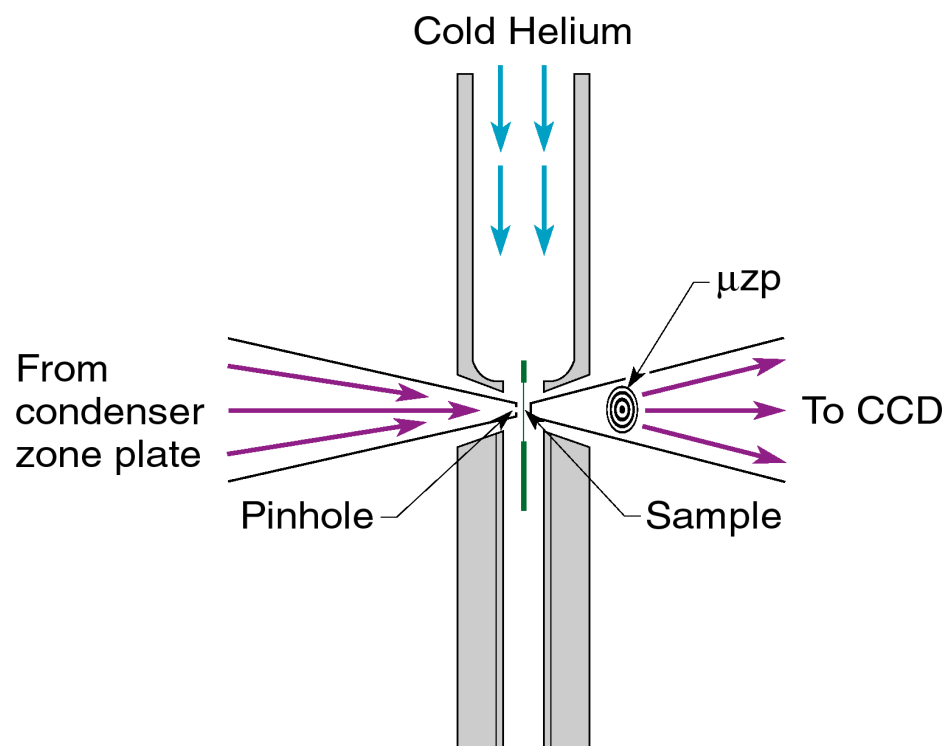


# The water window for biological x-ray microscopy



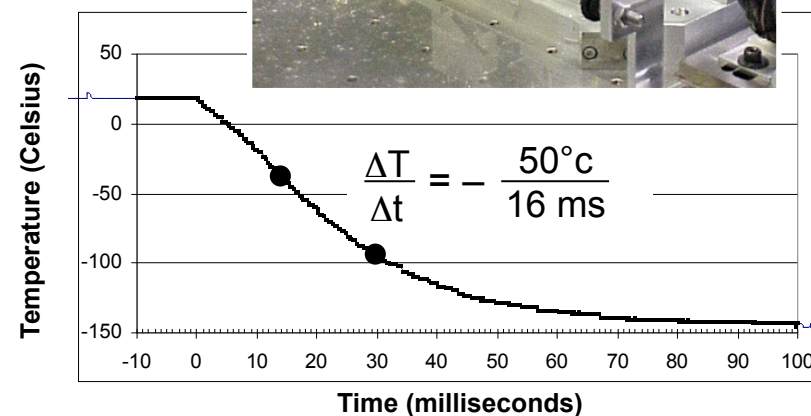
Ch09\_F25VG.ai

# Fast freeze cryo fixation strongly mitigates radiation dose effects



Helium passes through LN, is cooled, and directed onto sample windows

Fast Freeze

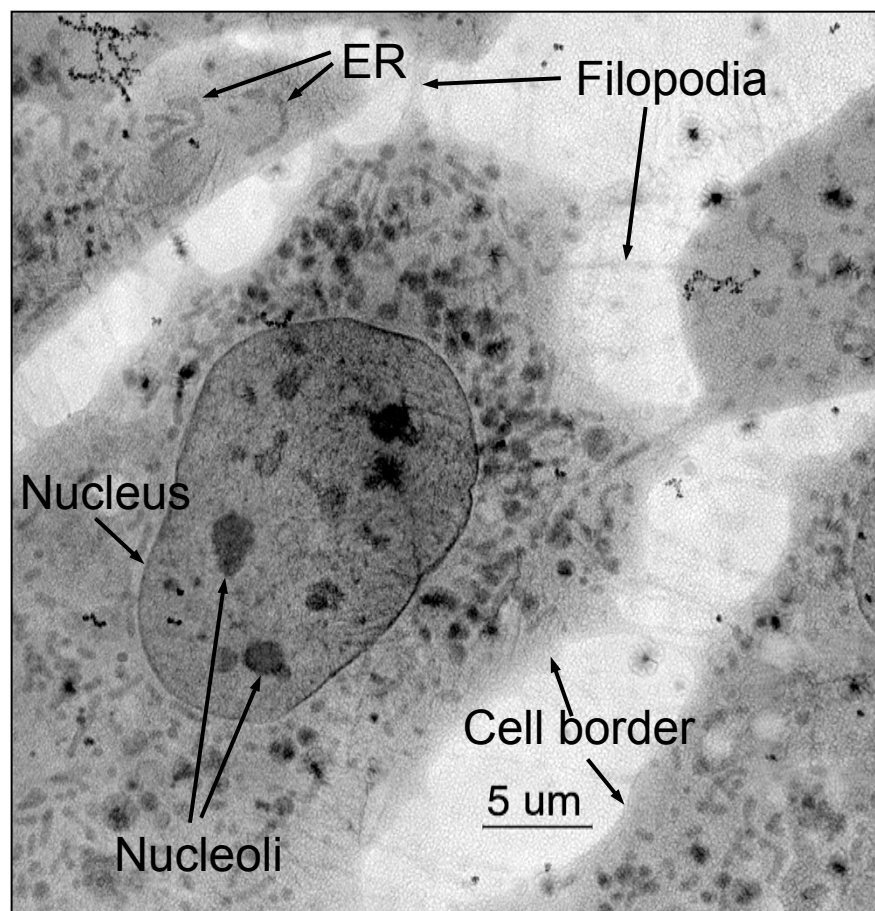


W. Meyer-Ilse, G. Denbeaux, L. Johnson, A. Pearson (CXRO-LBNL)



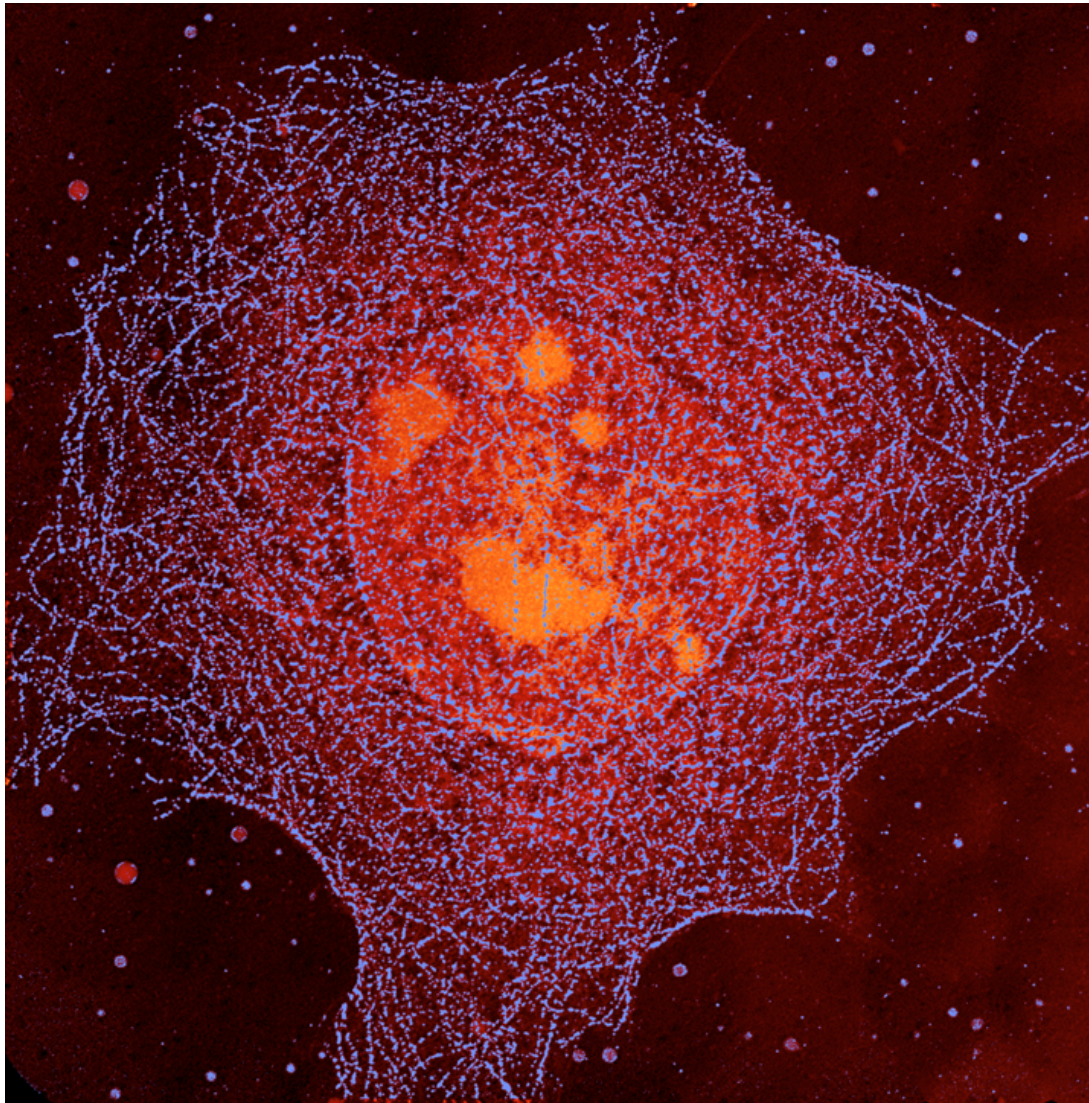
# Organelle details imaged with cryogenic preservation and high spatial resolution

## Cryo x-ray microscopy of 3T3 fibroblast cells



C. Larabell, D. Yager, D. Hamamoto, M. Bissell, T. Shin (LBNL Life Sciences Division)  
W. Meyer-Ilse, G. Denbeaux, L. Johnson, A. Pearson (CXRO-LBNL)

## Bending magnet radiation used with a soft x-ray microscope to form a high resolution image of a whole, hydrated mouse epithelial cell



$\hbar\omega = 520 \text{ eV}$

$32 \mu\text{m} \times 32 \mu\text{m}$

Ag enhanced Au labeling  
of the microtubule network,  
color coded blue.

Cell nucleus and nucleoli,  
moderately absorbing,  
coded orange.

Less absorbing aqueous  
regions coded black.

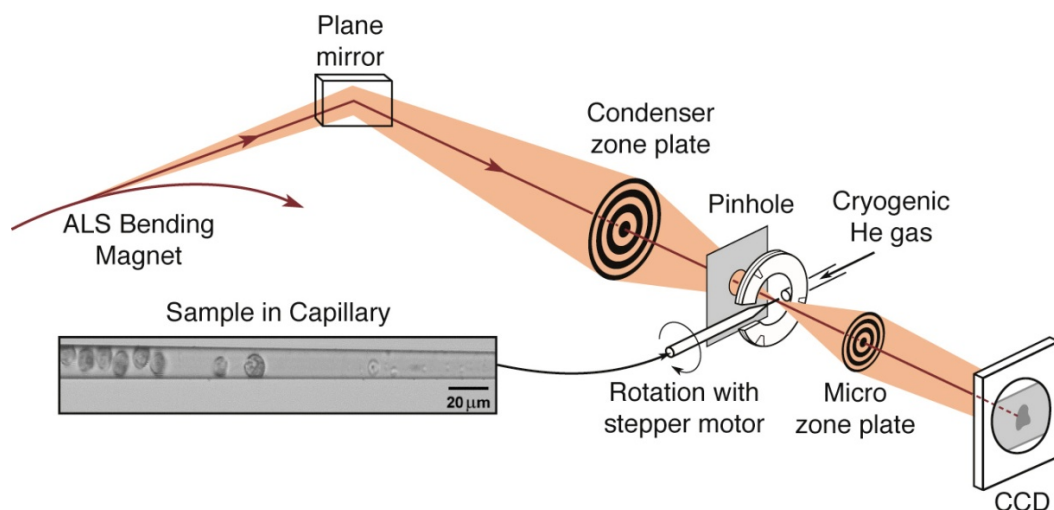
W. Meyer-Ilse et al.

J. Microsc. 201, 395 (2001)

Courtesy of C. Larabell and W. Meyer-Ilse (LBNL)

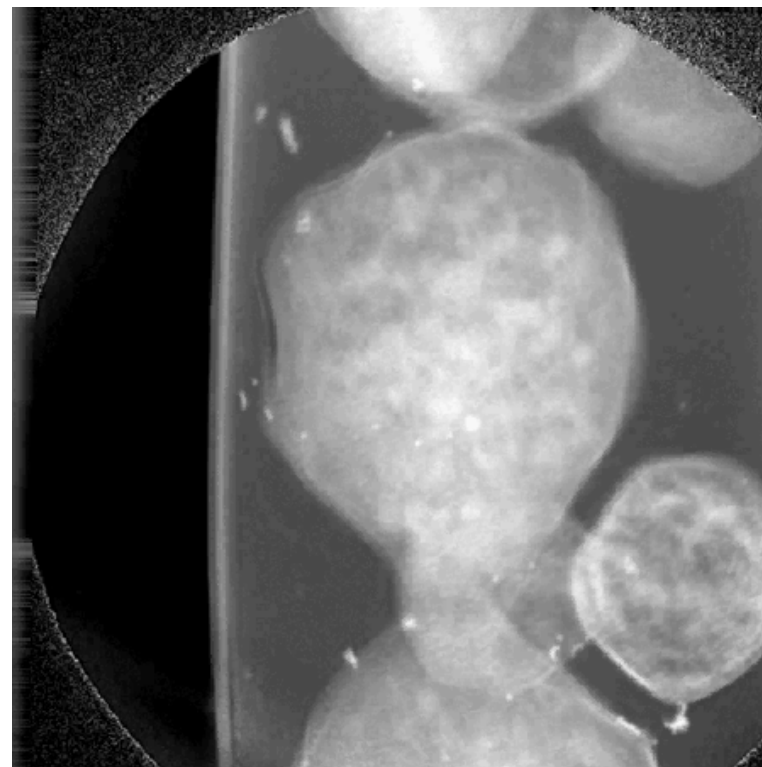


## Nanotomography of Cryogenic Fixed Cells



Courtesy of G. Schneider (BESSY)  
*Surf. Rev. Lett.* **9**, 177 (2002)

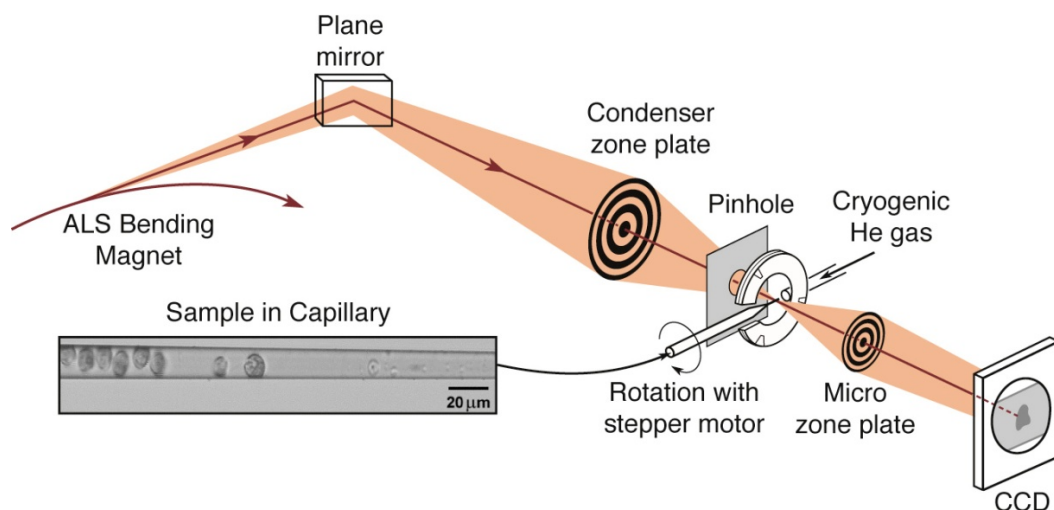
## Soft X-Ray Nanotomography of a Yeast Cell



$\lambda = 2.4 \text{ nm}$

Courtesy of C. Larabell (UCSF & LBNL)  
 and M. LeGros (LBNL)

## Nanotomography of Cryogenic Fixed Cells



$$\lambda = 2.4 \text{ nm (517 eV)}$$

$$\Delta r = 35 \text{ nm}$$

$$N = 320$$

$$NA = 0.034$$

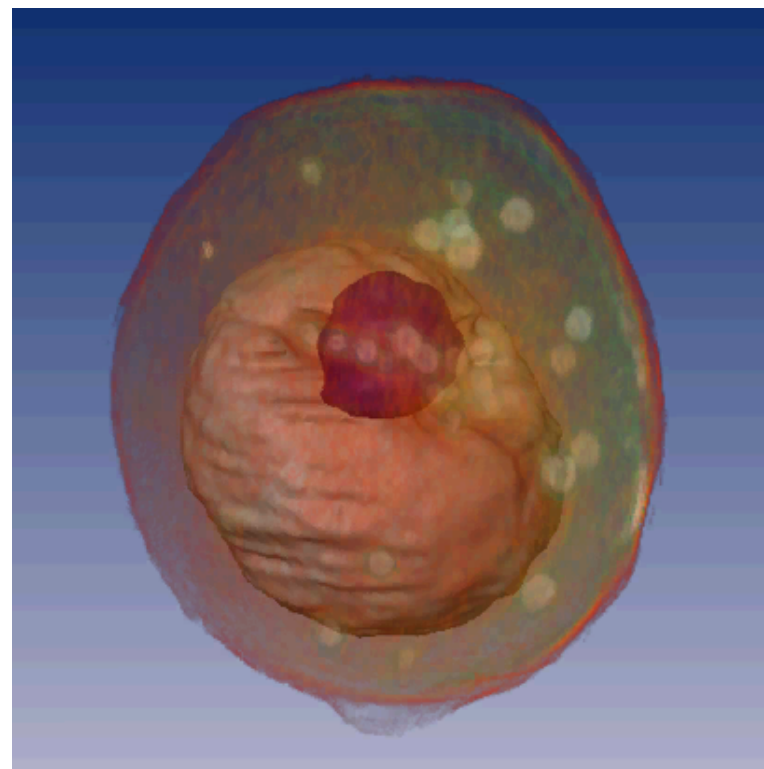
$$D = 45 \mu\text{m}$$

$$f = 650 \mu\text{m}$$

$$\sigma = 0.64$$

$$\text{Resolution} = 60 \text{ nm}$$

## Soft X-Ray Nanotomography of a Yeast Cell

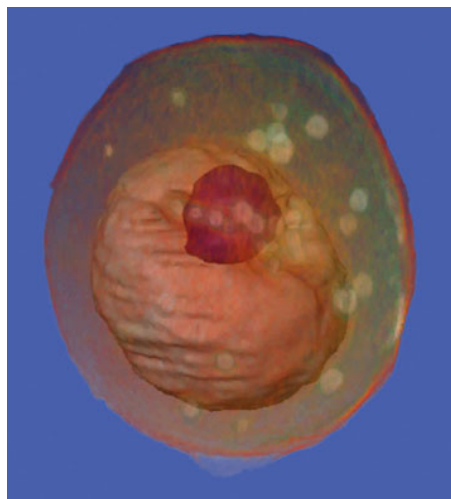


$$\lambda = 2.4 \text{ nm}$$

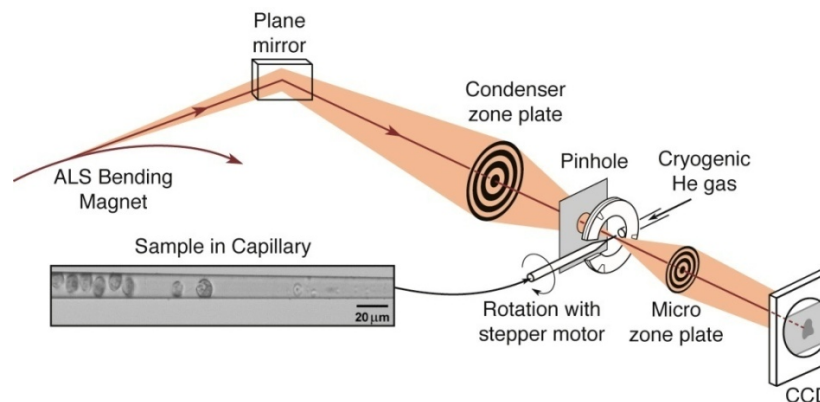
Courtesy of C. Larabell (UCSF & LBNL)  
and M. LeGros (LBNL)

UCSF NCXT

# Small DOF limits resolution for thick samples



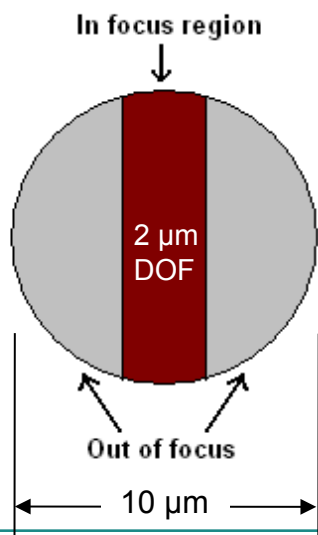
C. Larabell and M. LeGros,  
*Molec. Bio. Cell* 15, 957 (2004)



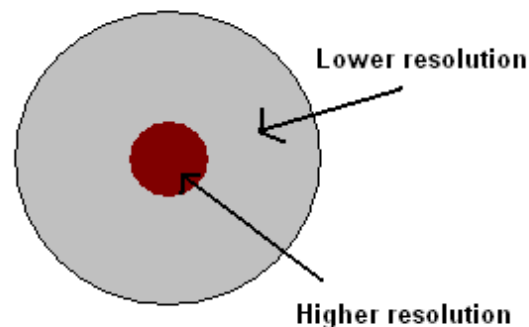
$$\text{Lateral Resolution} = \frac{k_1 \lambda}{NA} = 2k_1 \Delta r = \cancel{28 \text{ nm}} \quad 60 \text{ nm}$$

$$\text{Depth of field} = 2 \mu\text{m}$$

## Each projection image



## Reconstructed image

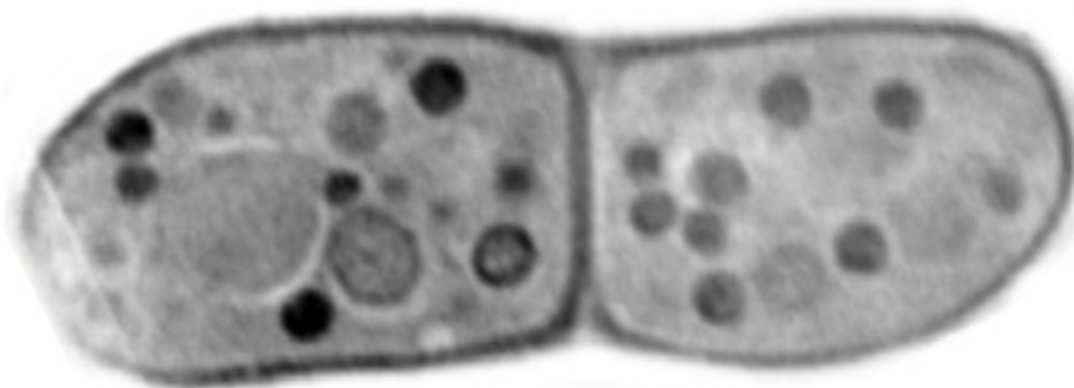


*Courtesy of Anne Sakdinawat (LBNL & UCB.)*

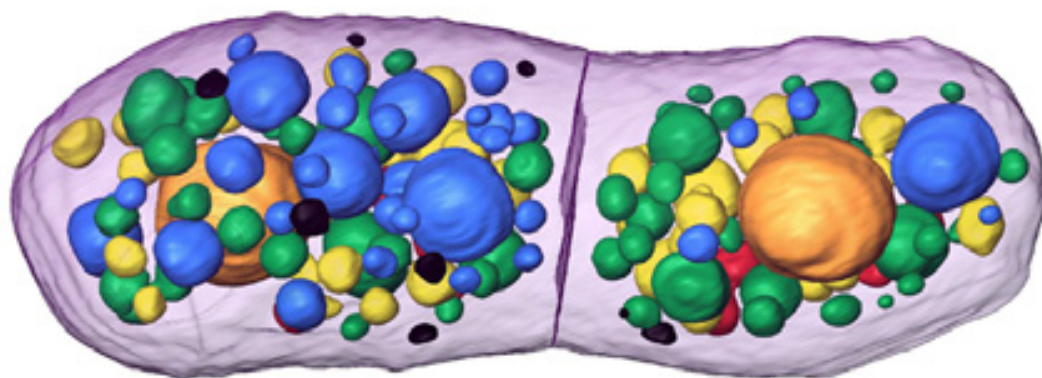


## Nanoscale 3-D biotomography

Mother daughter yeast cells just before separation



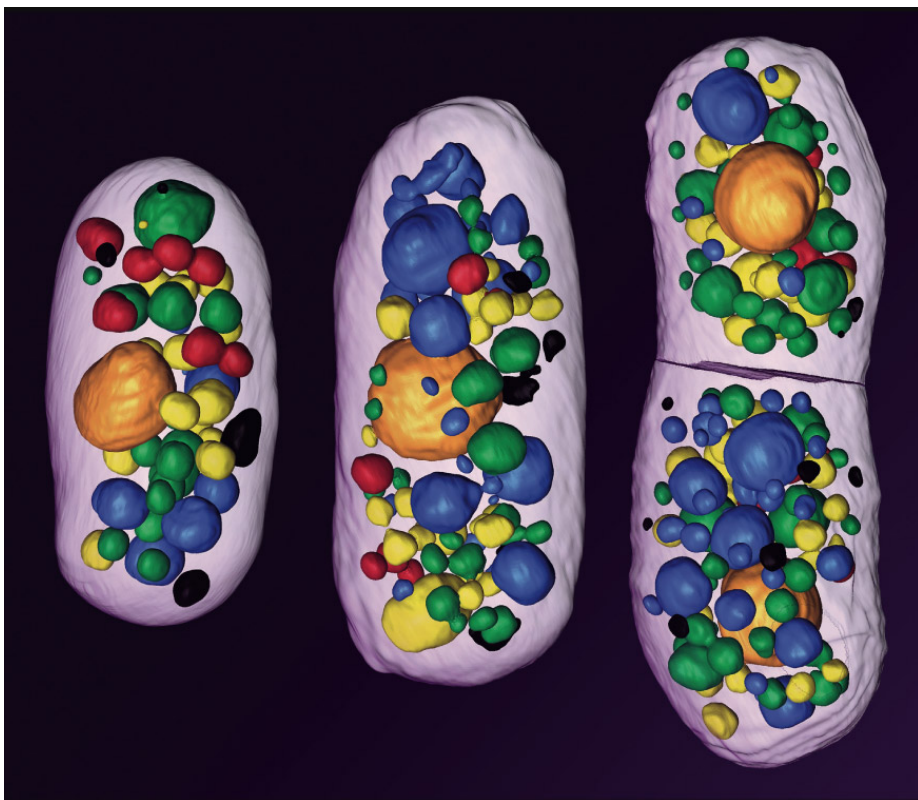
2-D slice from 3-D  
Tomogram. Images  
every 2°, 180° data  
set, several minutes.  
 $\Delta r = 45$  nm



Color coding  
identifies subcellular  
components by their  
x-ray absorption  
coefficients

Courtesy of Carolyn Larabell, UCSF/LBNL.

## Biotomography at 60 nm resolution



- Cryofixation
- 2° angular intervals
- Depth of focus limits resolution
- New XM-2 dedicated to biological applications, will become major facility worldwide to draw biologists to this evolving capability

Courtesy of C. Larabell (UCSF & LBNL)

UCSF NCXT

## High resolution (29 nm), 3D image of a mouse cell by soft x-ray tomography



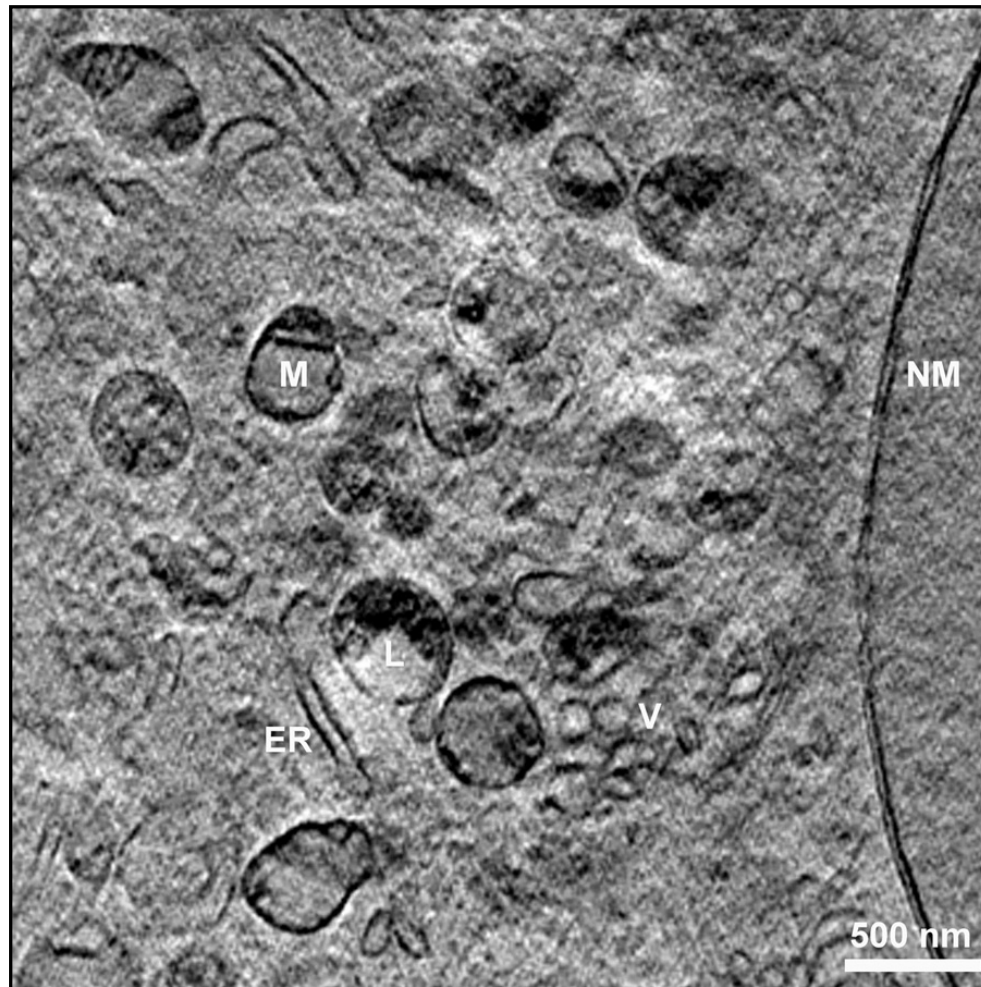
517 eV (2.4 nm)  
 $\Delta r = 25$  nm,  
1° intervals,  $\pm 60^\circ$   
29 nm nuclear  
double membrane.

Courtesy of  
Gerd Schneider, BESSYII  
and James McNally, NIH.



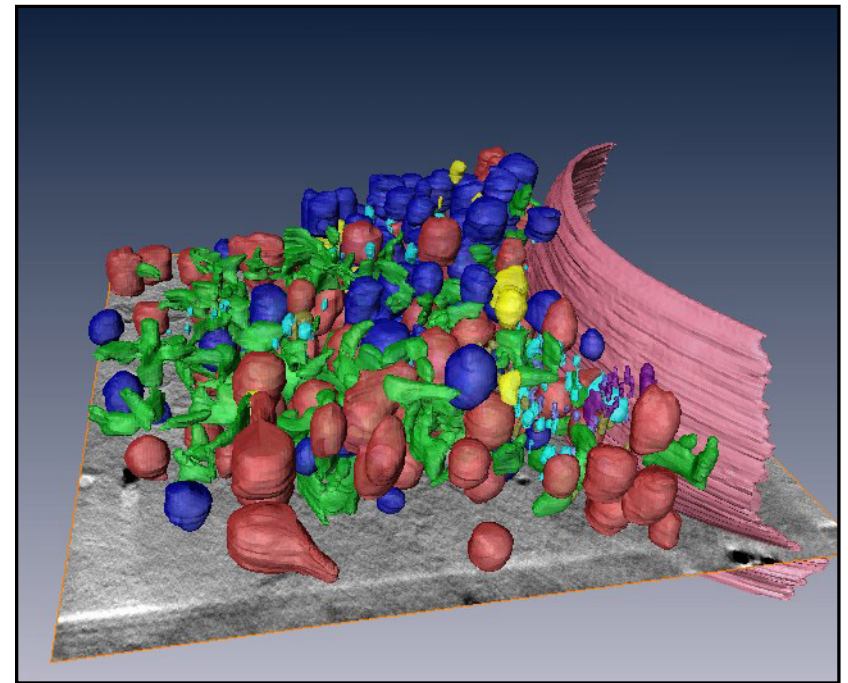
# High resolution (29 nm), 3D image of a mouse cell by soft x-ray tomography

2D slice from 3D data set



Details: 517 eV (2.4 nm)  
 $\Delta r = 25$  nm,  $1^\circ$  intervals,  $\pm 60^\circ$ .  
Note 29 nm nuclear membrane.

3D rendering



Courtesy of Gerd Schneider, BESSYII and James McNally, NIH.



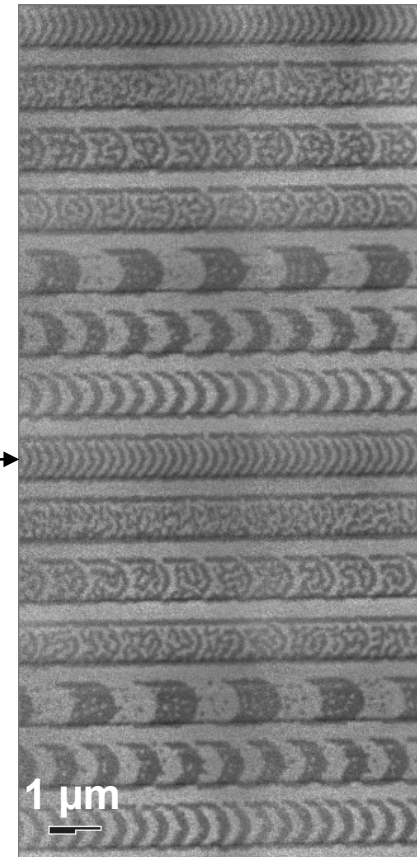
# Magnetic x-ray microscopy using x-ray magnetic circular dichroism (XMCD)



## Magnetic X-Ray Microscopy

- High spatial resolution in transmission
- Bulk sensitive (thin films)
- Complements surface sensitive PEEM
- Good elemental sensitivity
- Good spin-orbit sensitivity
- Allows applied magnetic field
- Insensitive to capping layers
- In-plane and out-of-plane measurements

100 nm  
lines &  
spaces



Courtesy of P. Fischer, (MPI, Stuttgart) and G. Denbeaux (CXRO/LBNL)



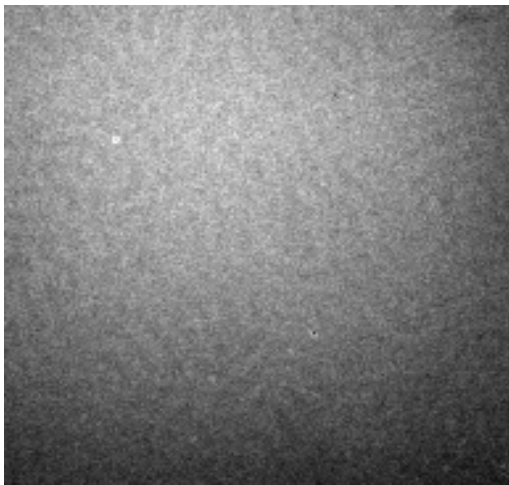


# Magnetic domains imaged at different photon energies

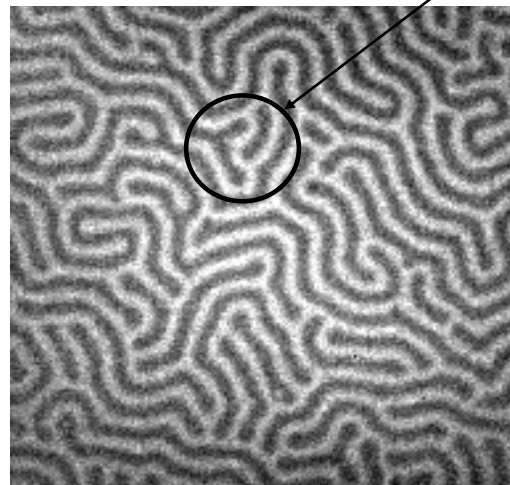


## FeGd Multilayer

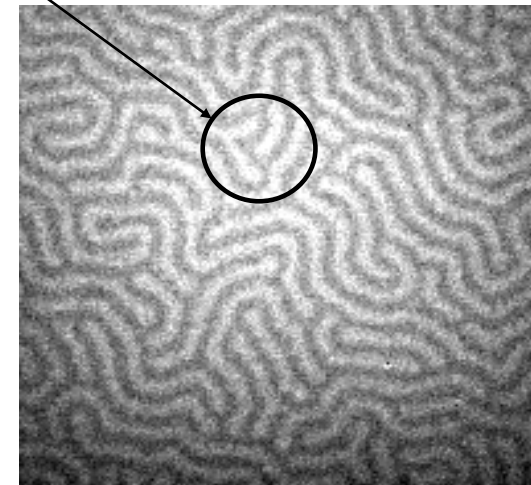
1  $\mu\text{m}$



$\hbar\omega = 704 \text{ eV}$   
below Fe L-edges



$\hbar\omega = 707.5 \text{ eV}$   
Fe L<sub>3</sub>-edge

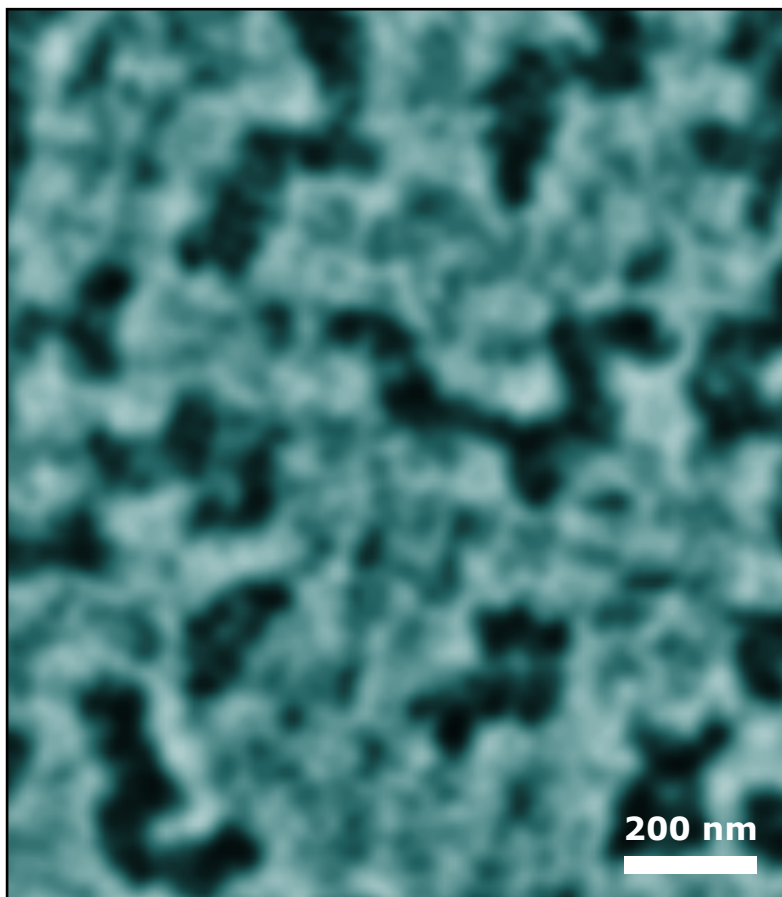


$\hbar\omega = 720.5 \text{ eV}$   
Fe L<sub>2</sub>-edge

Contrast reversal

P. Fischer, T. Eimüller, M. Koehler (U. Würzburg)  
S. Tsunashima (U. Nagoya) and N. Tagaki (Sanyo)  
G. Denbeaux, L. Johnson, A. Pearson (CXRO-LBNL)

# Magnetic recording of nanomagnetic patterns to 15 nm spatial resolution



CoCrPt alloy  
Co L<sub>3</sub>-edge at 778 eV  
(1.59 nm)

Courtesy of Peter Fischer (LBNL)

P. Fischer et al., *Mat. Today* 9, 26 (2006).

# Time resolved studies of vortex dynamics in patterned permalloy thin films

Pump and Probe setup requires:

- Pump: Current pulse to “pump” sample
- Probe: X-ray pulses (70ps) from ALS 2 Bunch mode
- Perfect repeatability of dynamics



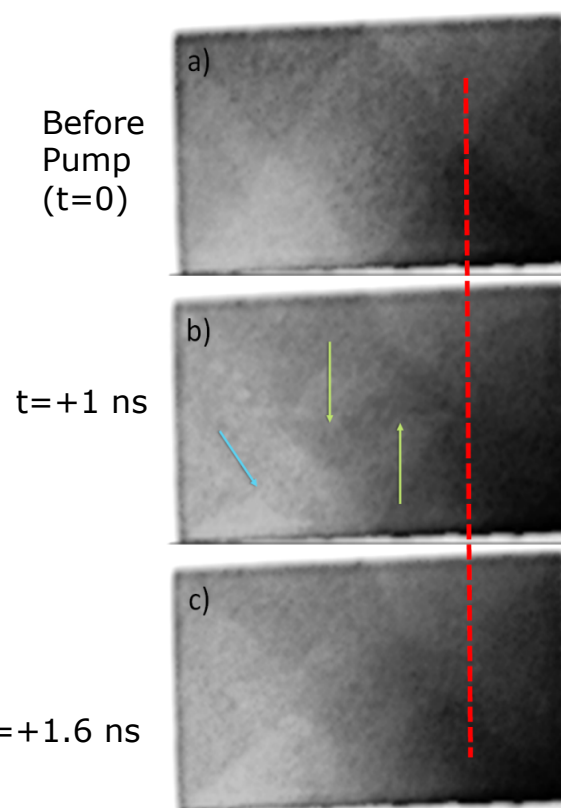
*B.L. Mesler, P. Fischer, W. Chao, E. H. Anderson, D.H. Kim J. Vac. Sci. Technol. B 25, 2598 (2007).*

## Sample:

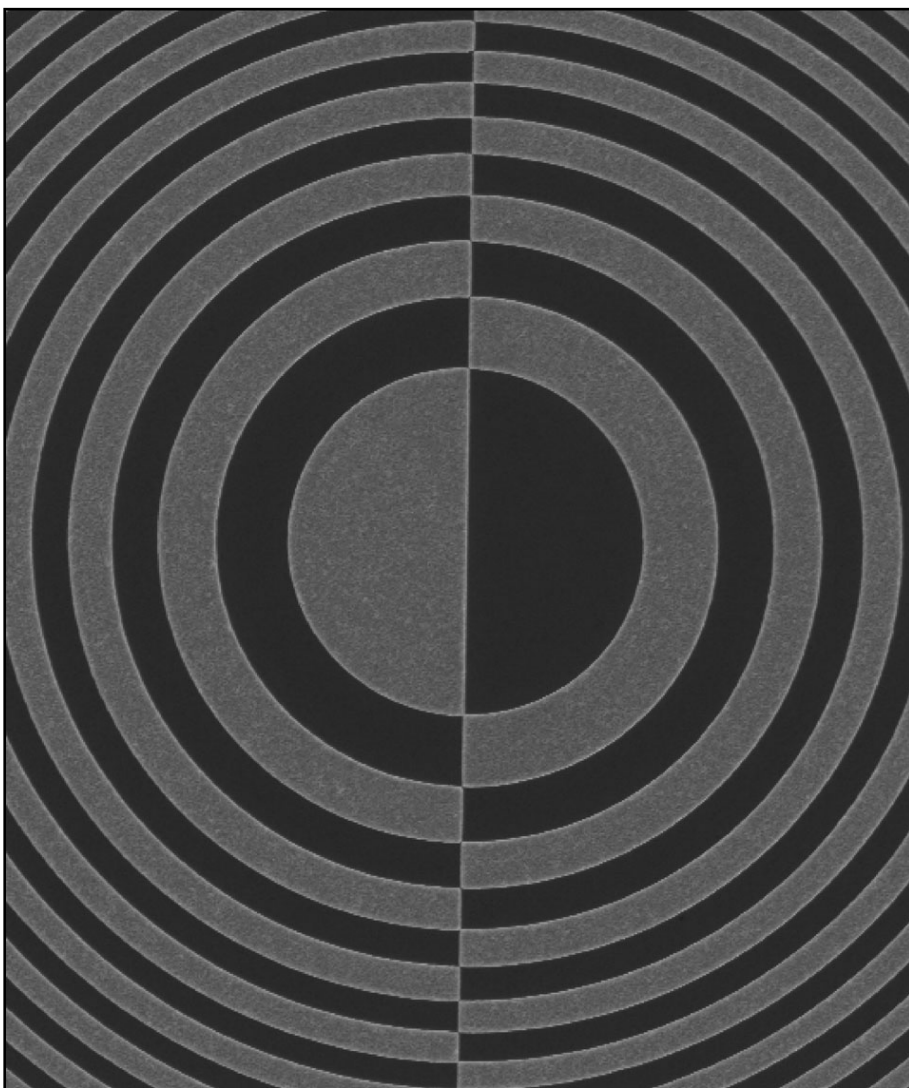
50 nm thick  $2\mu\text{m} \times 4\mu\text{m}$  permalloy ( $\text{Ni}_{80}\text{Fe}_{20}$ )

100nm thick gold waveguide

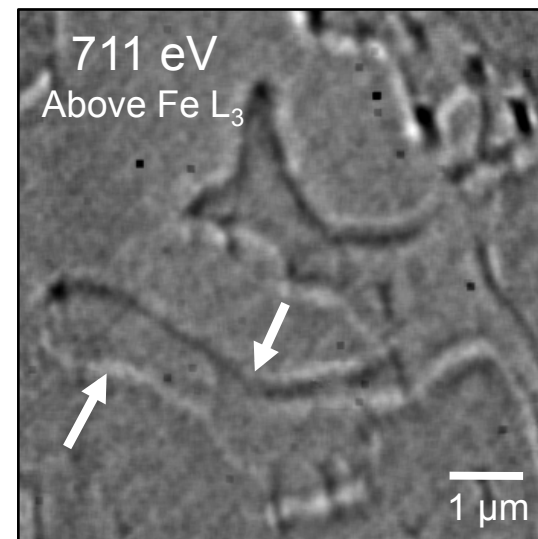
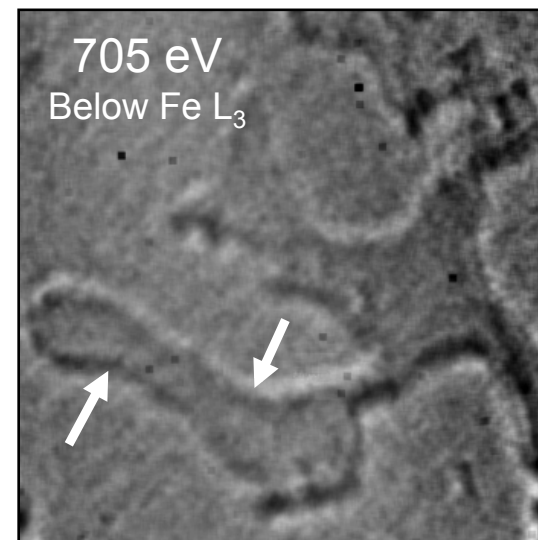
( $\Delta I$  along waveguide generates field to pump sample)



# Differential interference contrast (DIC) imaging at nanoscale magnetic edges



XOR Zone plate



59 nm thick  $\text{Gd}_{25}\text{Fe}_{75}$  layer

Courtesy of A. Sakdinawat, C. Chang and P. Fischer.





# Environmental Consequences of Portland cement

1.5 billion ton of cement

**Problem!**

**Generates 1.5 billion  
ton of CO<sub>2</sub>**

**Responsible for 7%  
CO<sub>2</sub> production in  
the world**

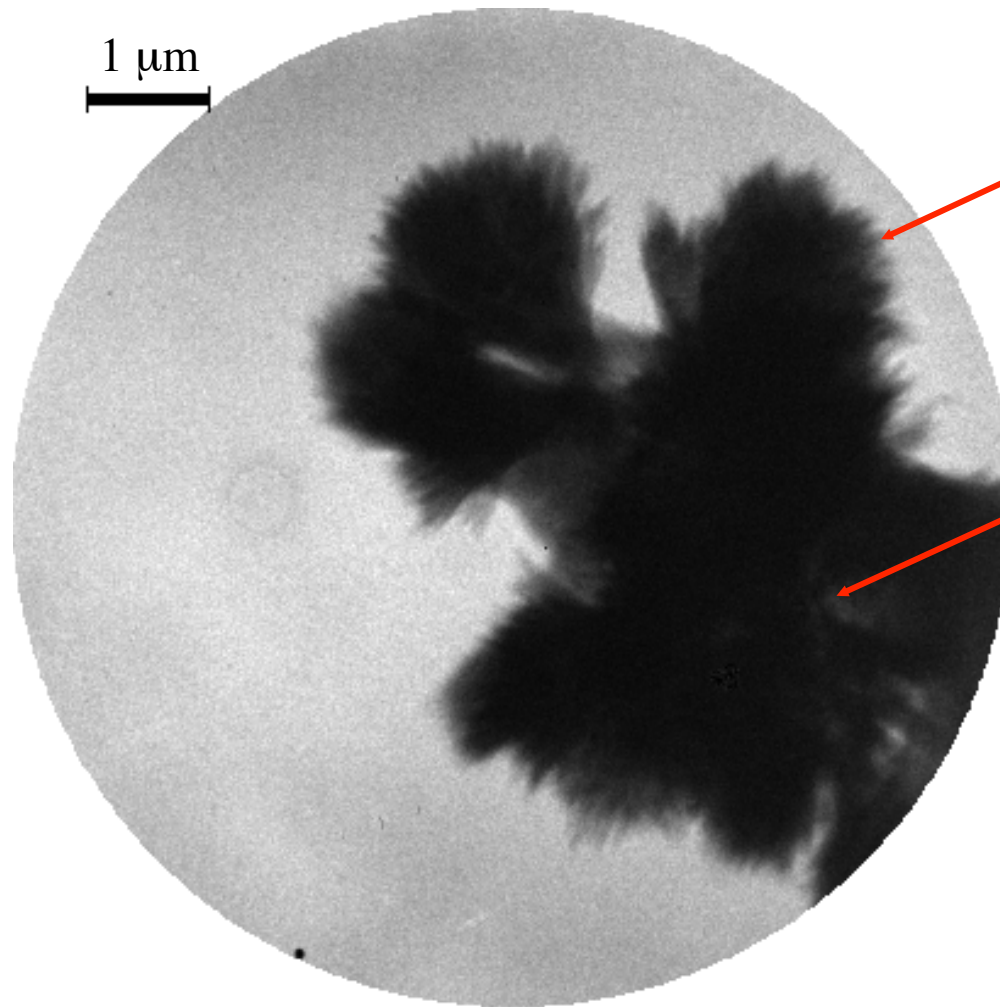


Courtesy of Professor Paulo Monteiro, CEE, UC Berkeley





## Nanoscale x-ray imaging of cement processes: early hydrates forming during the pre-induction period



Early hydrates  
(Sheaf of wheat)

Grain

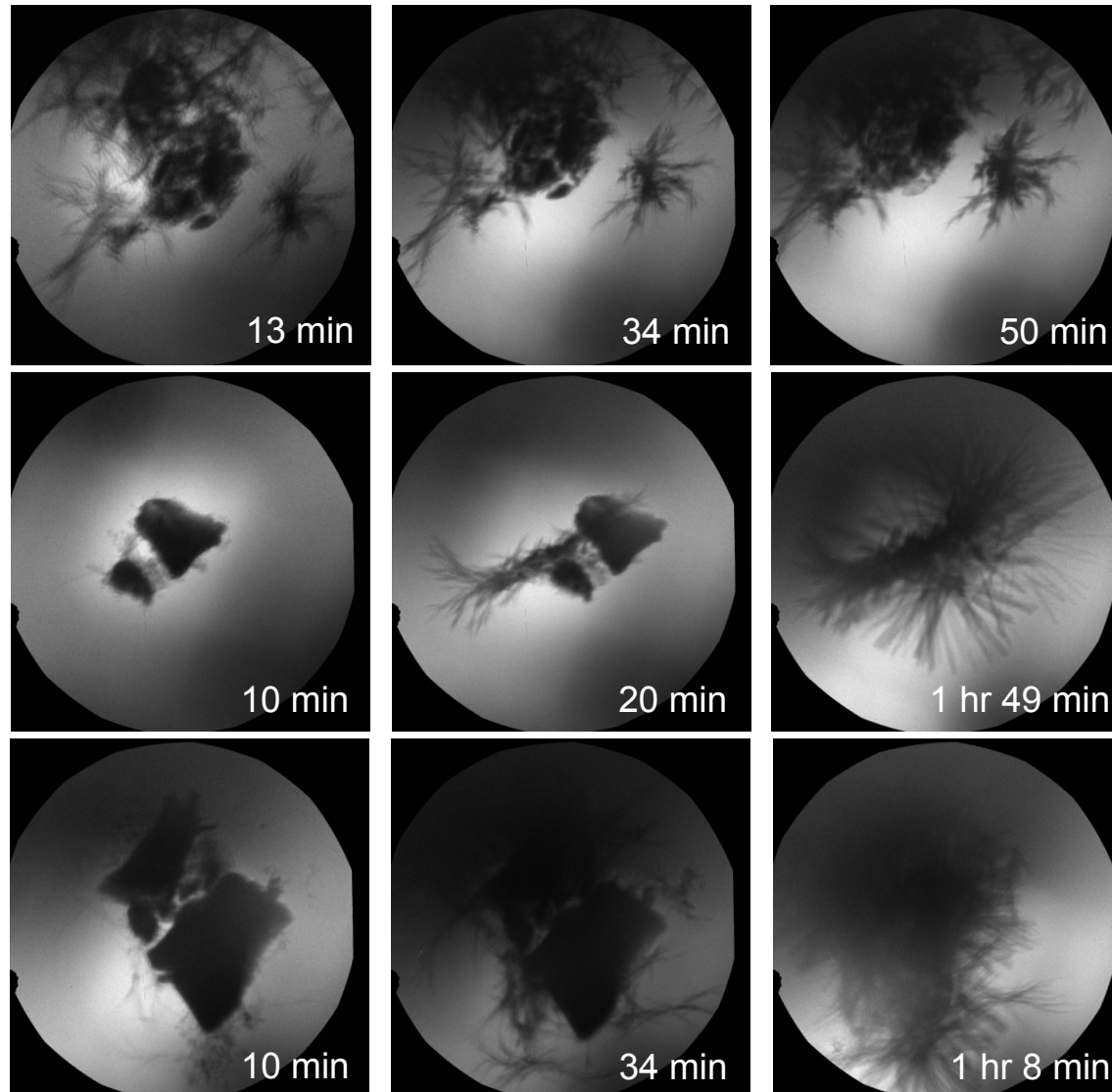
C3S hydrated for 34 min. in  
saturated lime and calcium  
sulfate at  $w/c = 5$ , 1 s  
exposure time, 516 eV, scale  
bar 1 μm.

Courtesy of Professor Paulo Monteiro, CEE, UC Berkeley



# Nanoscale x-ray imaging of cement processes

Calcium-Silicate-Hydrate (C-S-H): critical to cement strength and durability.



Orth  $C_3A$

Orth  $C_3A$  + 1%  $CaCl_2$

Orth  $C_3A$  + accelerator

C: carbon

Ca: calcium

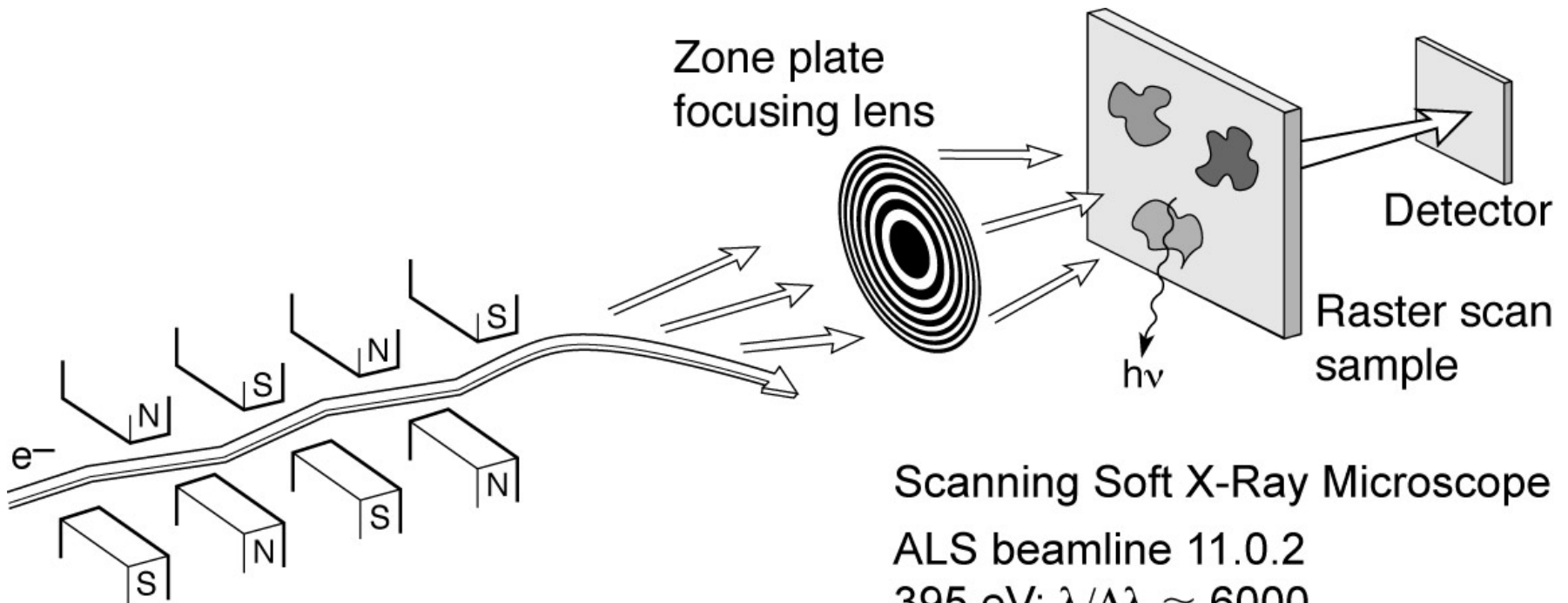
A: alumina ( $Al_2O_3$ )

S: silica ( $SiO_2$ )

520 eV, 40 nm - spatial resolution

Courtesy of Professor Paulo Monteiro, CEE, UC Berkeley

# Spectromicroscopy: high spatial and high spectral resolution of surface and thin films



## Scanning Soft X-Ray Microscope

ALS beamline 11.0.2

395 eV;  $\lambda/\Delta\lambda \approx 6000$

240 × 240 pixels

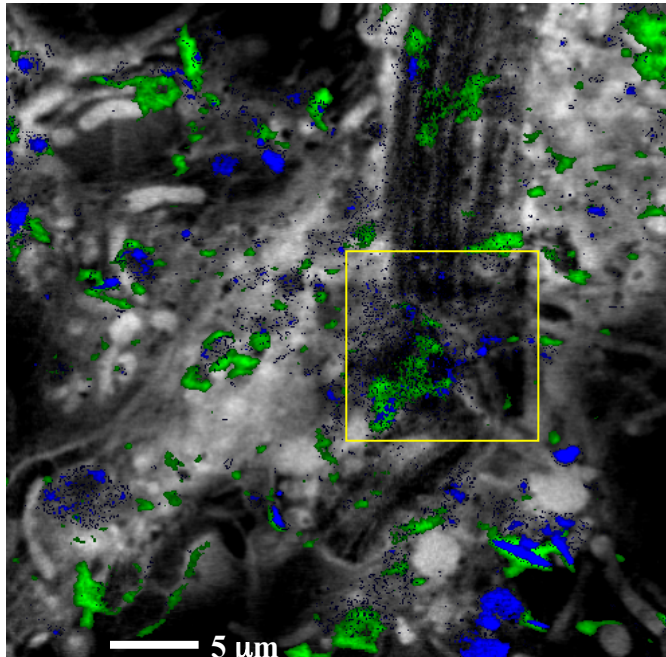
1.2  $\mu\text{m}$  × 1.2  $\mu\text{m}$

2 ms dwell time

Ch09\_F40a\_Feb2010.ai



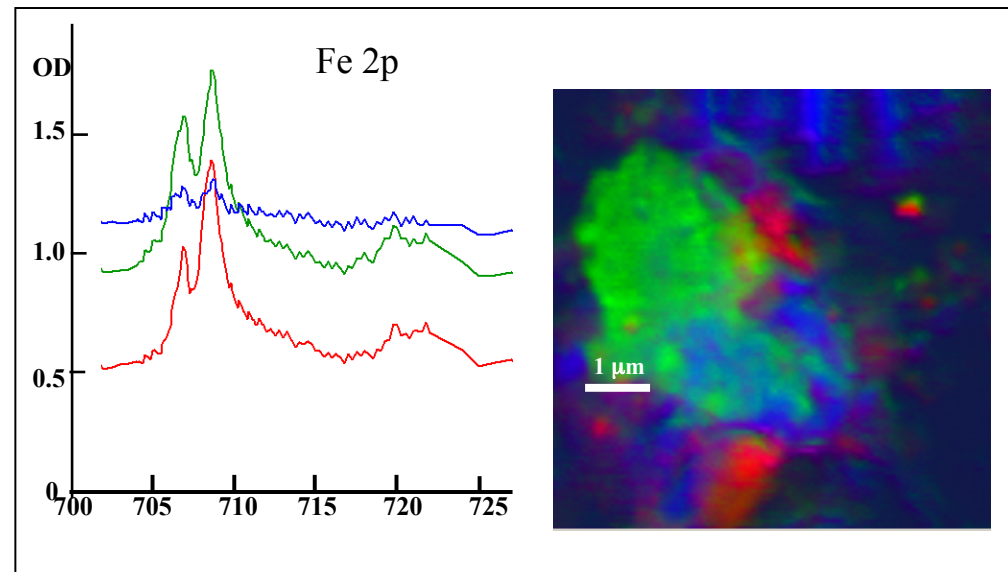
# Biofilm from Saskatoon River



Protein (gray), Ca, K

## RESULTS

- Ni, Fe, Mn, Ca, K, O, C elemental map, (there was no sign of Cr.)
- Different oxidation states for Fe and Ni



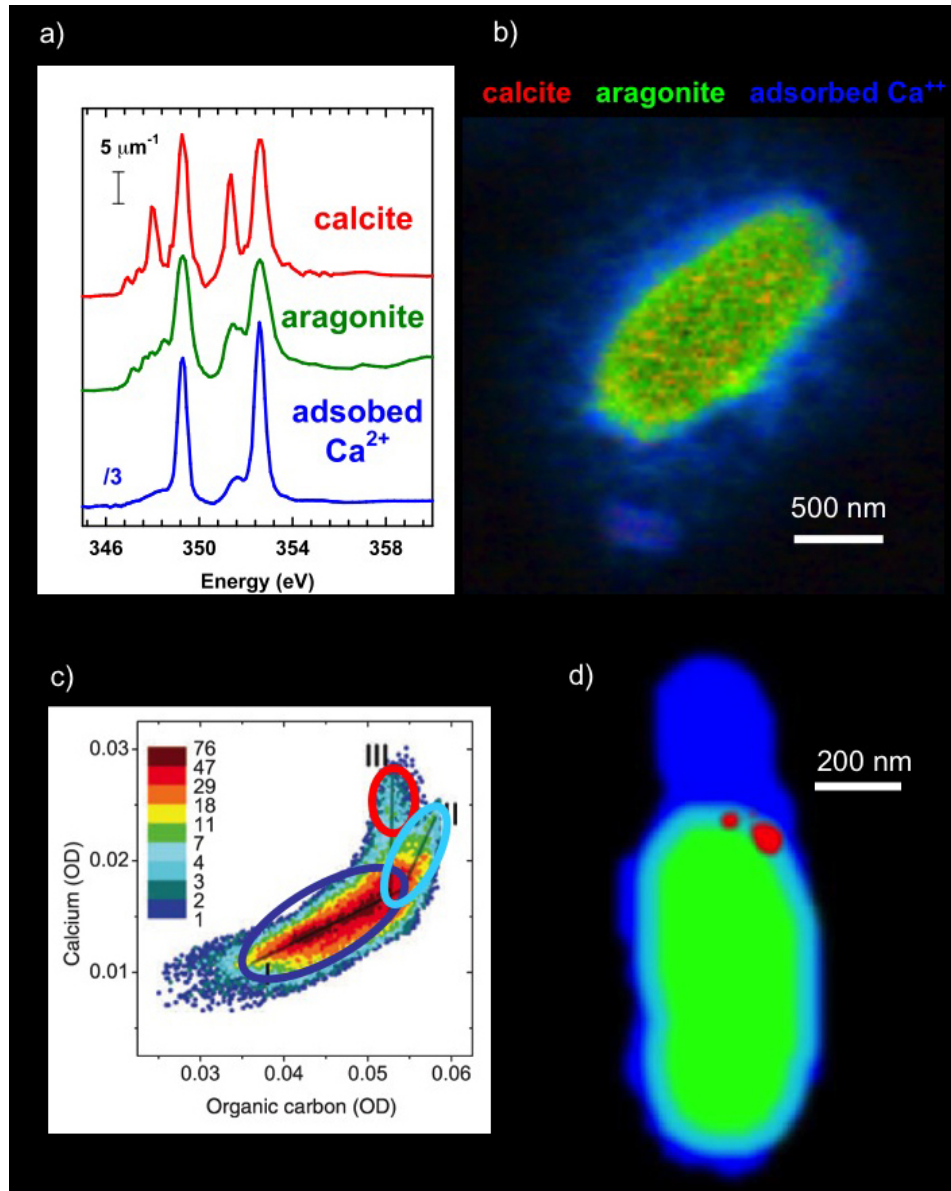
*Different oxidation states (minerals) found for Fe & Ni*

Tohru Araki, Adam Hitchcock (McMaster University)

Tolek Tyliczszak, LBNL

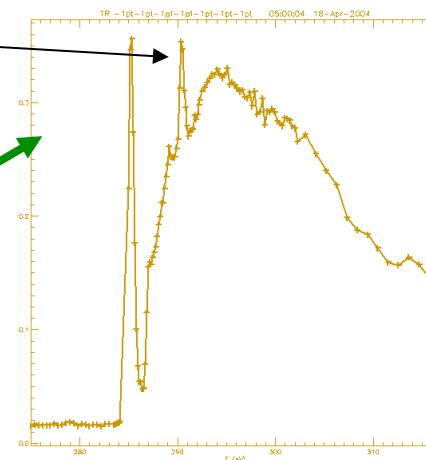
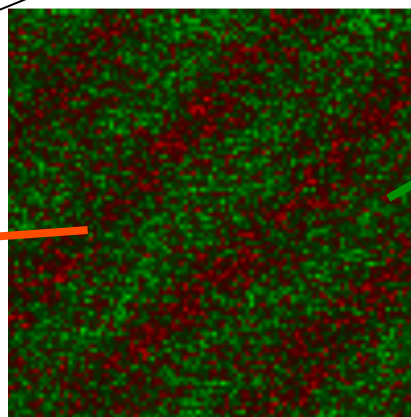
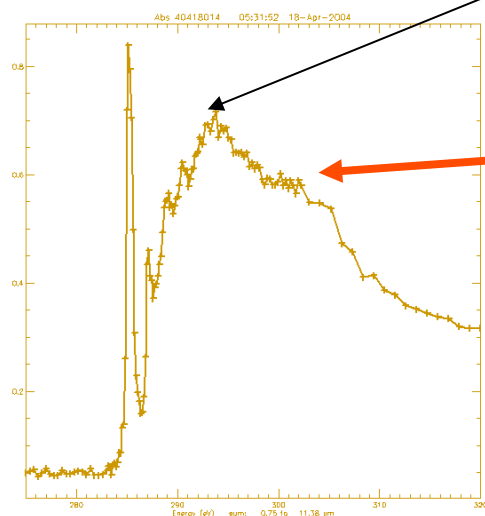
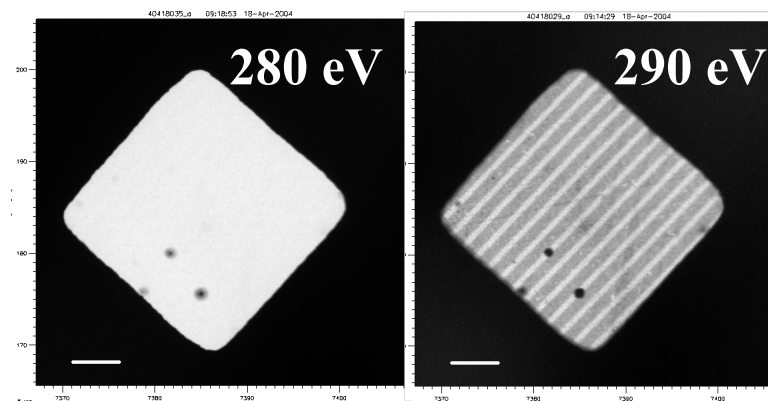
Sample from: John Lawrence, George Swerhone (NWRI-Saskatoon), Gary Leppard (NWRI-CCIW)

# A. Hitchcock, McMaster U.



M.K. Gilles, R. Planques, S.R. Leone  
LBNL  
Samples from B. Hinsberg, F. Huele  
IBM Almaden

## Exposure to UV light results in loss of carbonyl peak



Map chemical spectra taken of pure samples onto a sample containing both components

Courtesy of Mary Gilles, LBNL



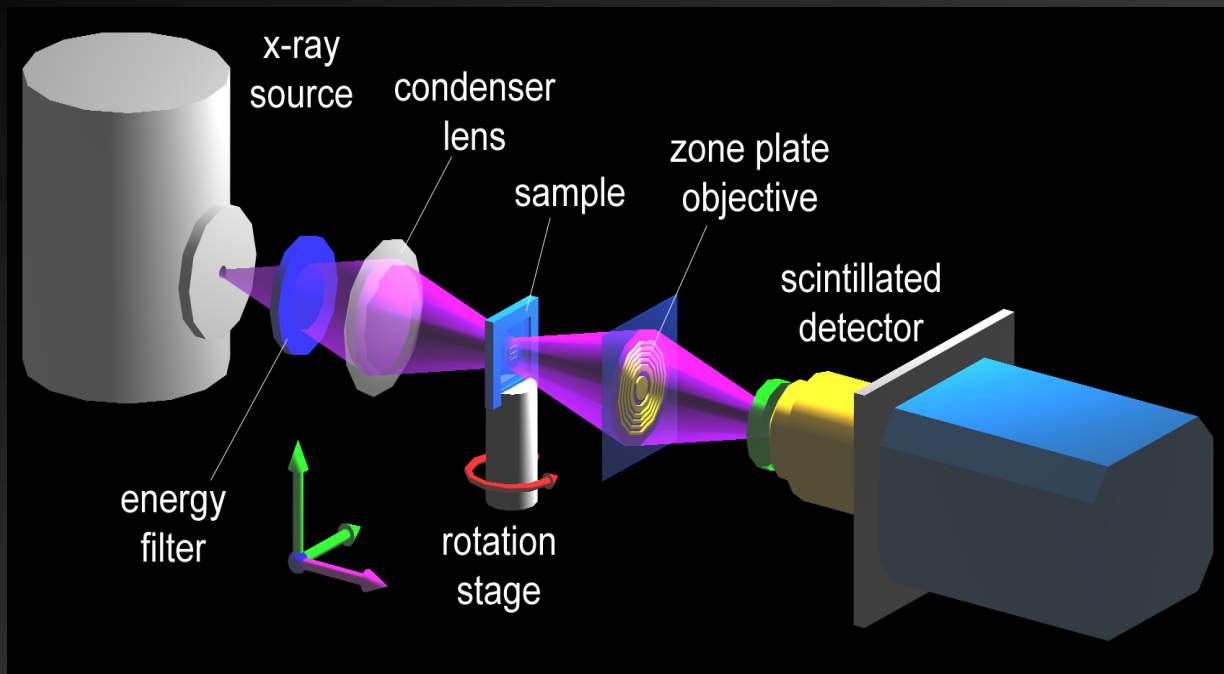
# Hard x-ray zone plate microscopy

---

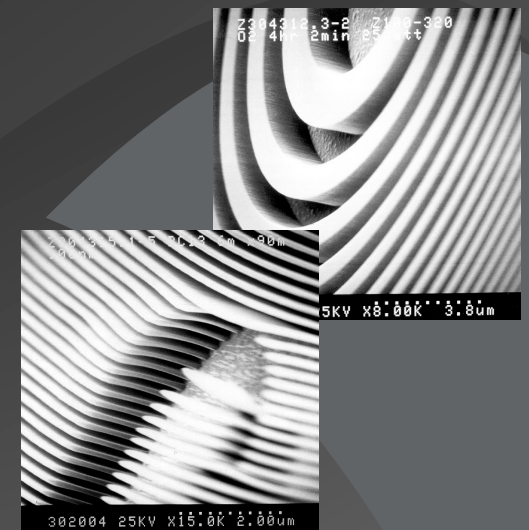


- Shorter wavelengths, potentially better spatial resolution and greater depth-of-field.
- Less absorption ( $\beta$ ); phase shift ( $\delta$ ) dominates, higher efficiency.
- Thicker structures required (e.g., zones), higher aspect ratios pose nanofabrication challenges.
- Contrast of nanoscale samples minimal; will require good statistics, uniform background, dose mitigation.

# nanoXCT: Schematic and Challenges



## X-ray Zone-plate Lens



Challenges for achieving nm scale resolution:

- High resolution objective lens: limiting the ultimate resolution
- High numerical aperture condenser lens:
- Detector: high efficiency for lab. source and high speed for synchrotron sources
- Precision mechanical system

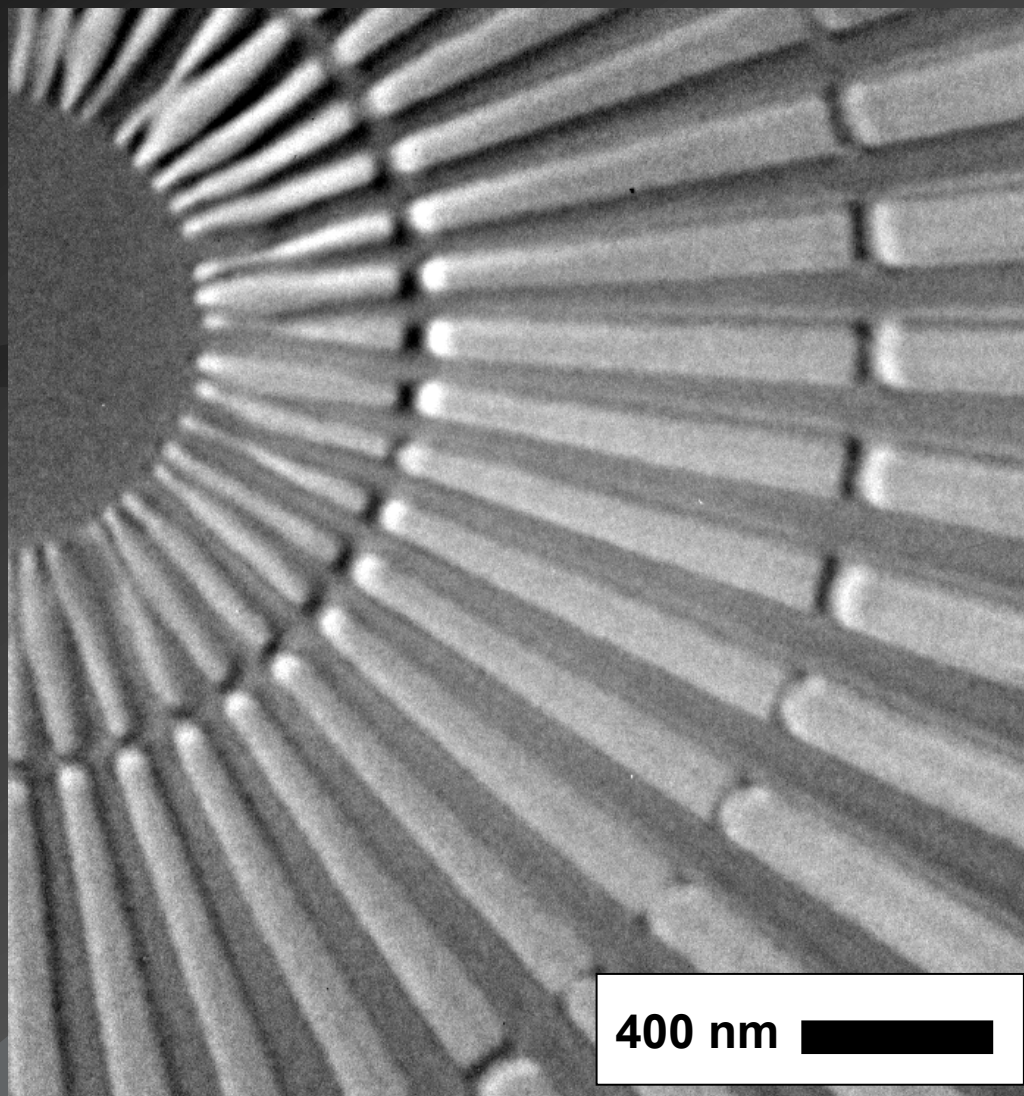
# Xradia nanoXCT: Sub-25 nm Hard X-ray Image

## Xradia Resolution Pattern

- 50 nm bar width
- 150 nm thick Au
- 8keV x-ray energy
- 3<sup>rd</sup> diffraction order

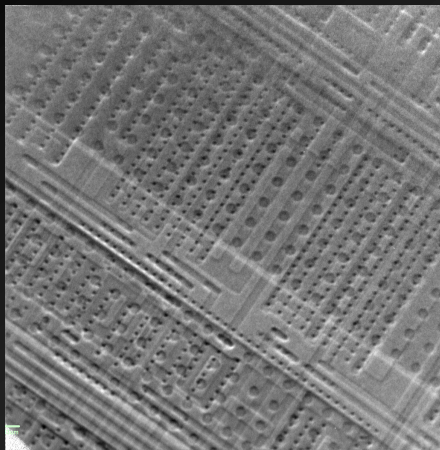
F. Duewer, M. Tang,  
G. C. Yin, W. Yun,  
M. Feser, et al.

Xradia nano-XCT  
8-50S installed at  
NSRRC, Taiwan

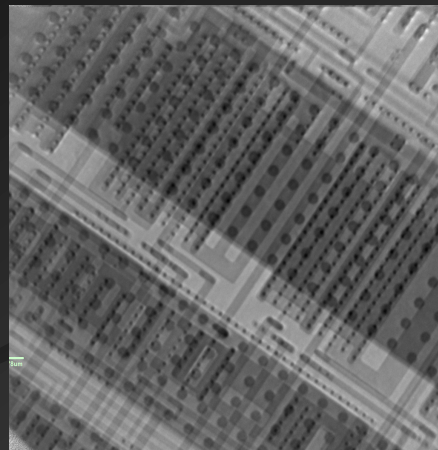




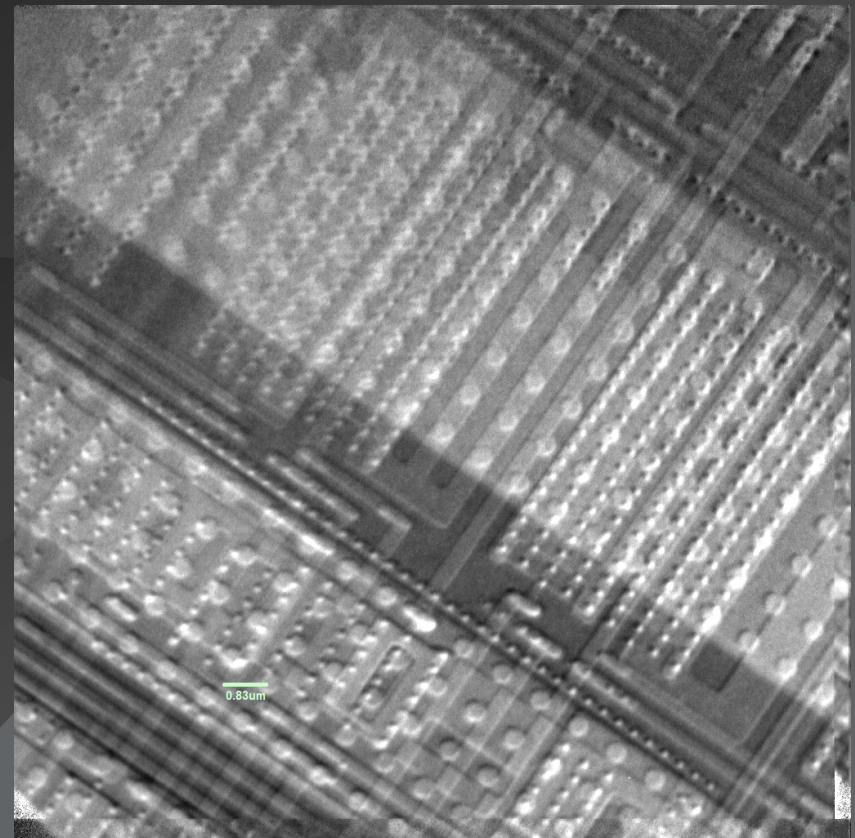
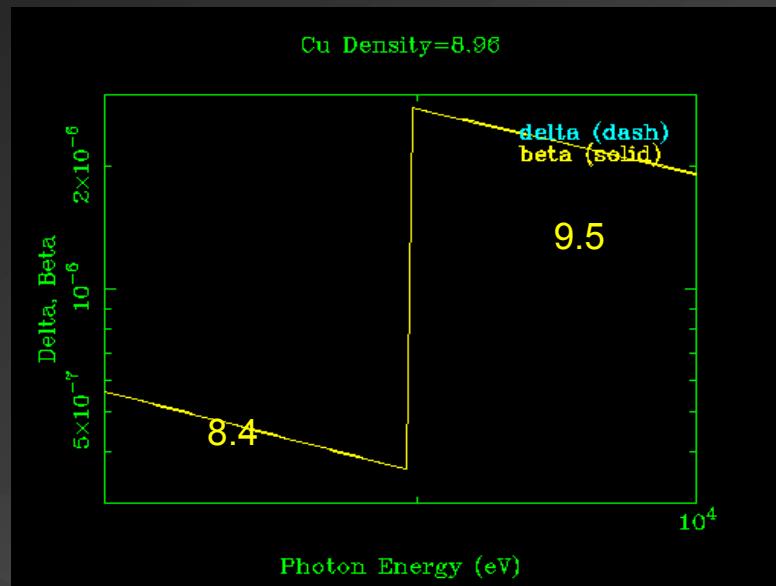
# Elemental contrast by tuning energy across the copper absorption edge ( Guan-Chian Yin *et al*)



8.4 keV

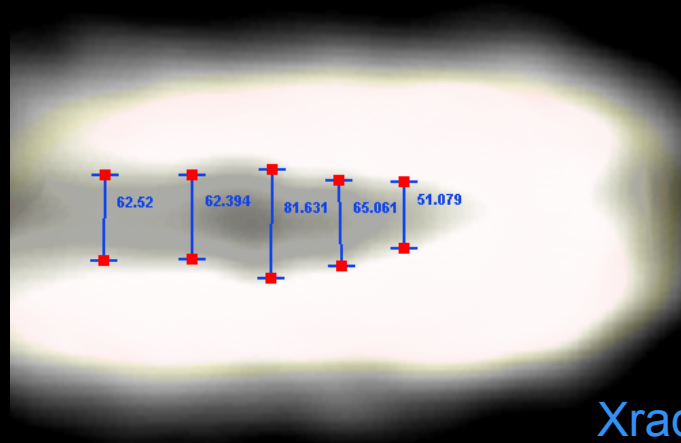
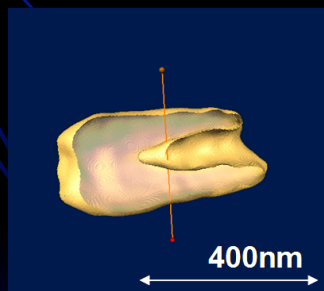
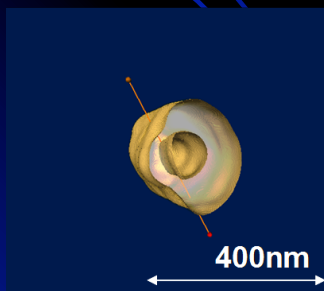
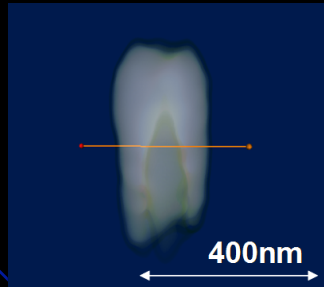
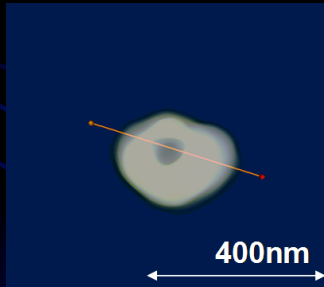
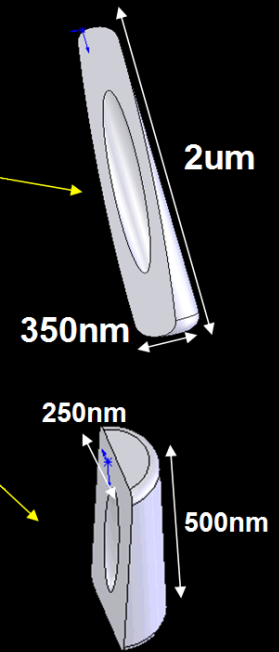
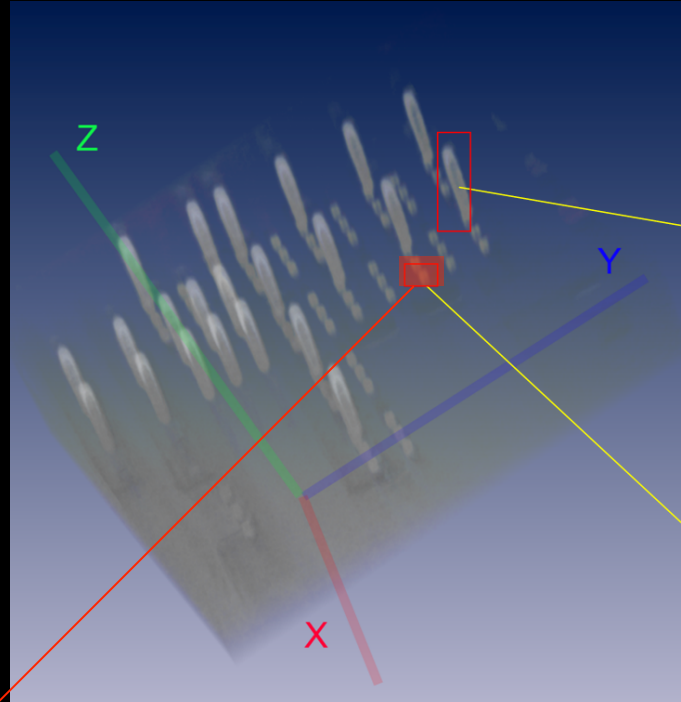
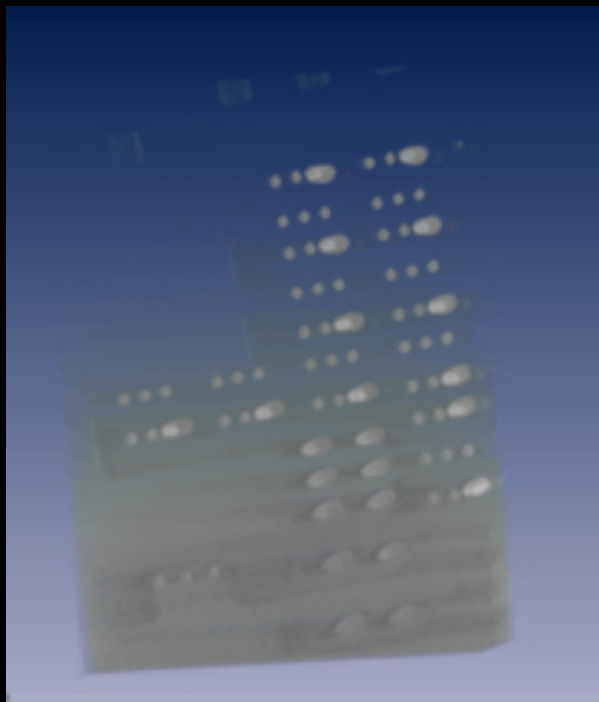


9.5 keV



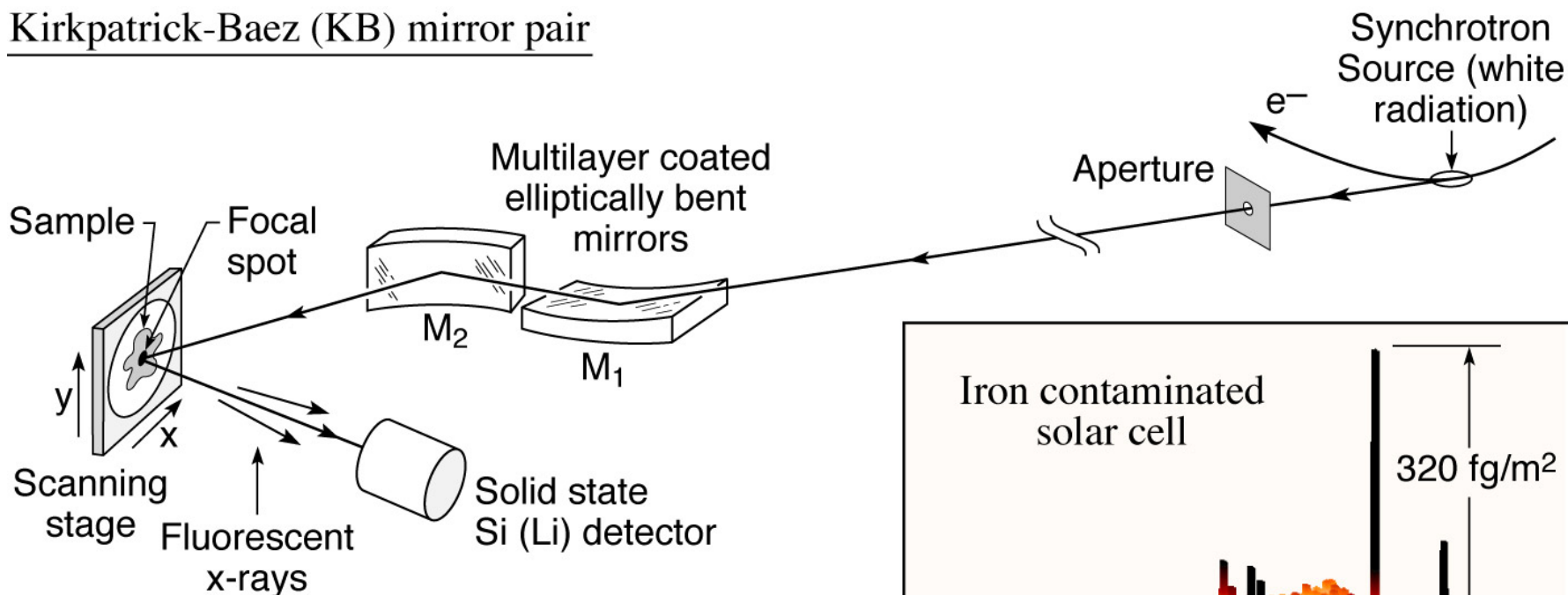
Intensity difference between  
 $E = 8.4$  keV and 9.5 keV

# Tomography of a Tungsten plug with "keyhole" at ~60 nm spatial resolution

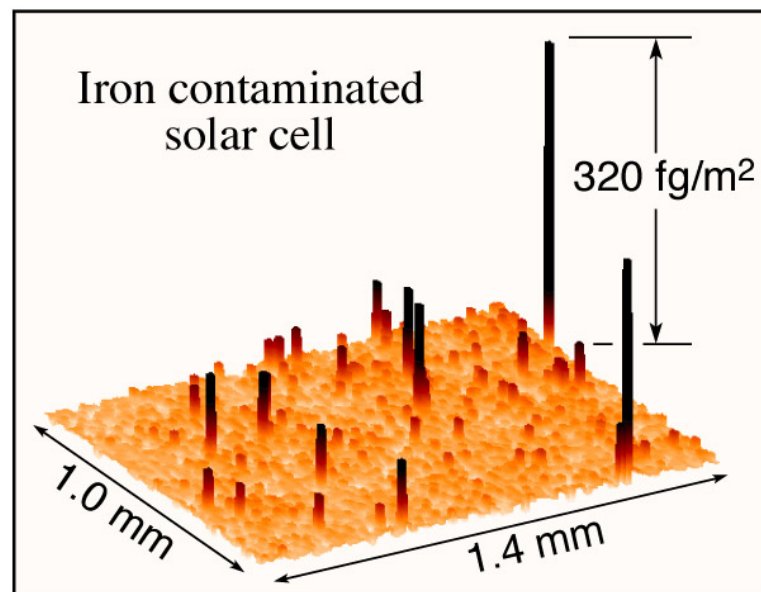


Xradia and NSRRC  
APL. 88, 241115 (2006)

## Kirkpatrick-Baez (KB) mirror pair



- Crossed cylinders at glancing incidence
- Photon in / photon out, low noise background
- Femtogram and part per billion (ppb) sensitivity
- Micron focus (1988), now  $\sim 25$  nm (Yamauchi, Mimura and colleagues, Osaka U./Spring-8)



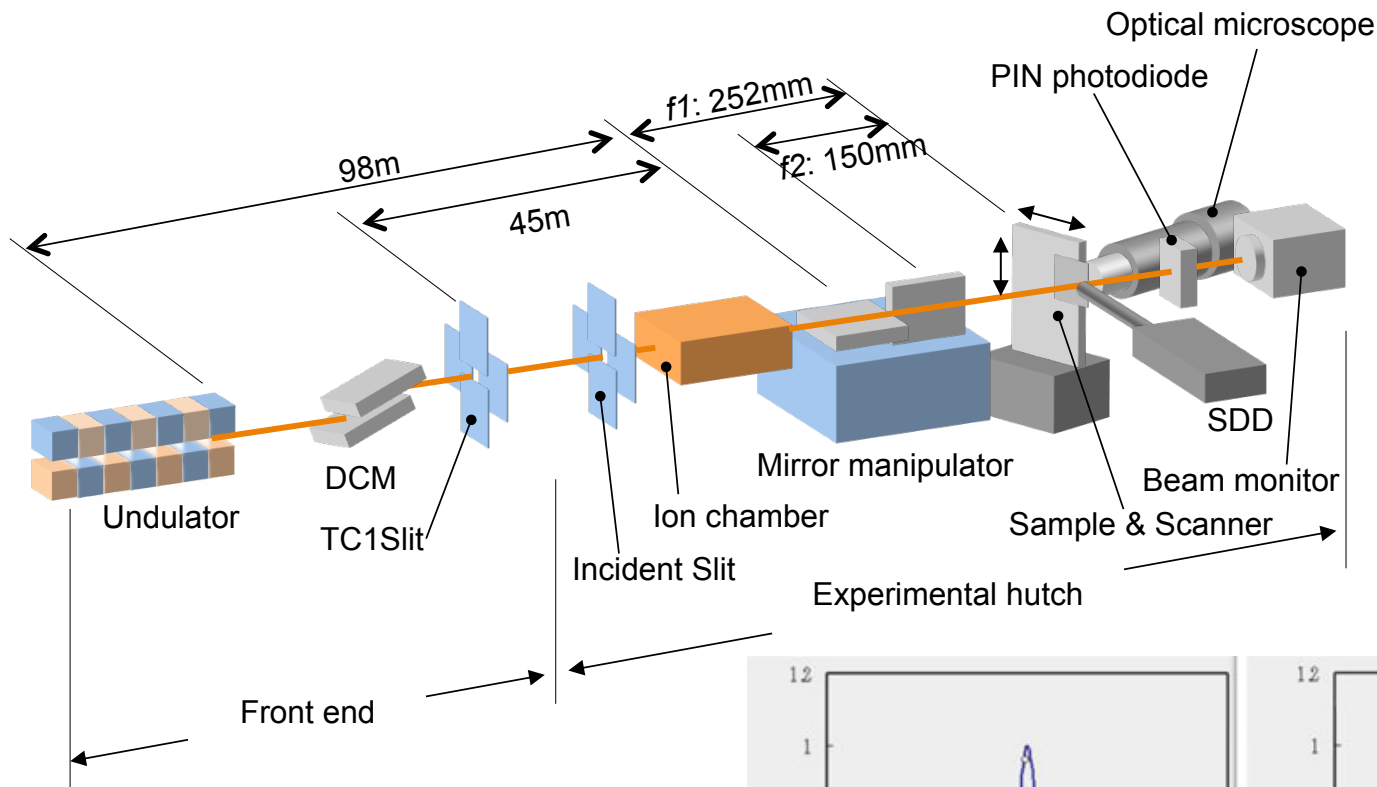
(Courtesy of A. Thompson and J. Underwood, LBNL; and R. Holm, Miles Lab)

FluoresMicroprobe\_Sept2010.ai

J.H. Underwood and A.C. Thompson, NIM A266, 296 & 318 (1988).

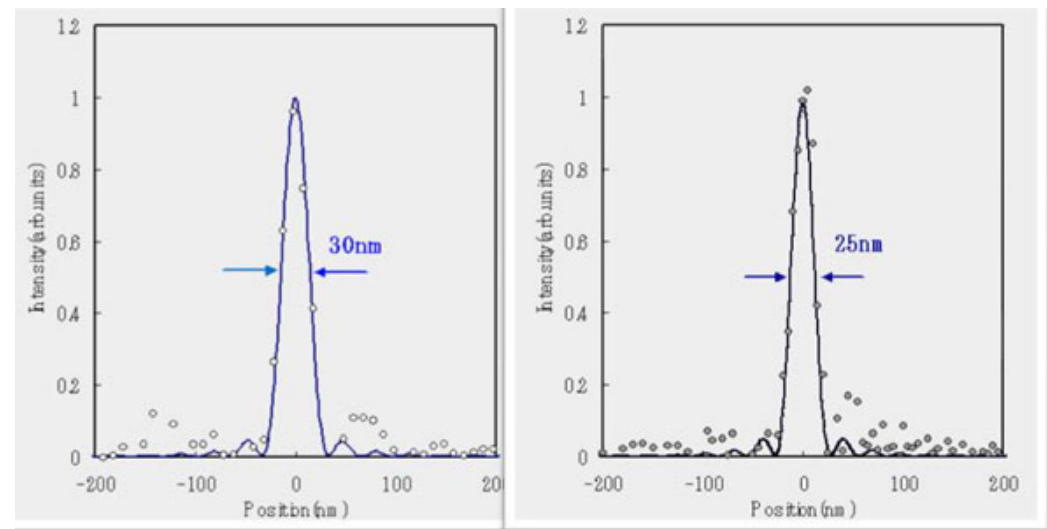


# X-ray microprobe at SPring-8

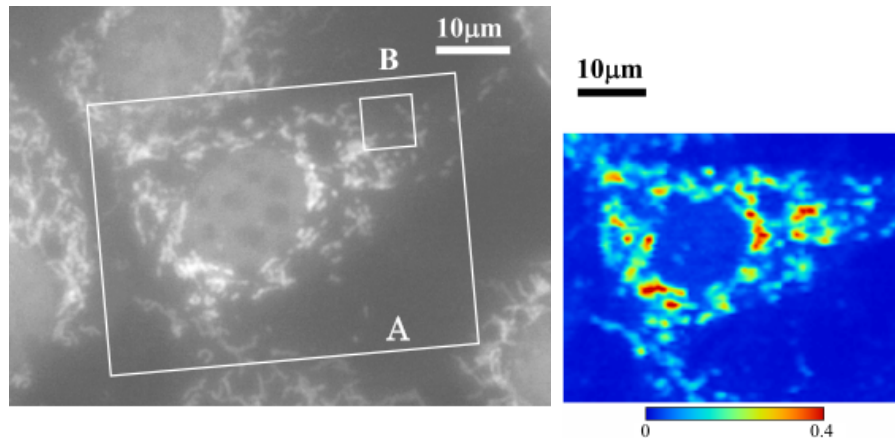


S. Matsuyama et al.,  
Rev. Sci. Instrum.  
77, 103102 (2006)

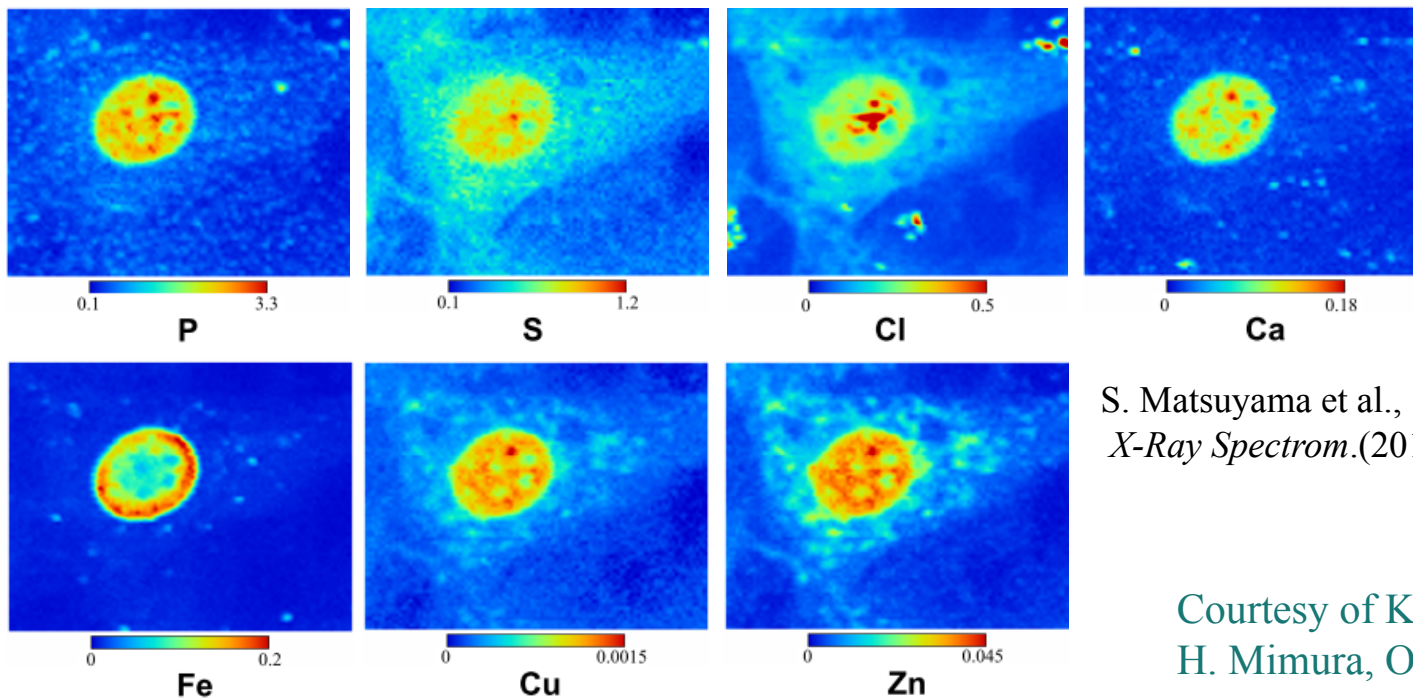
Courtesy of K. Yamauchi and  
H. Mimura, Osaka University.



# Sub-cellular elemental analysis using the hard x-ray fluorescence microprobe at SPring-8



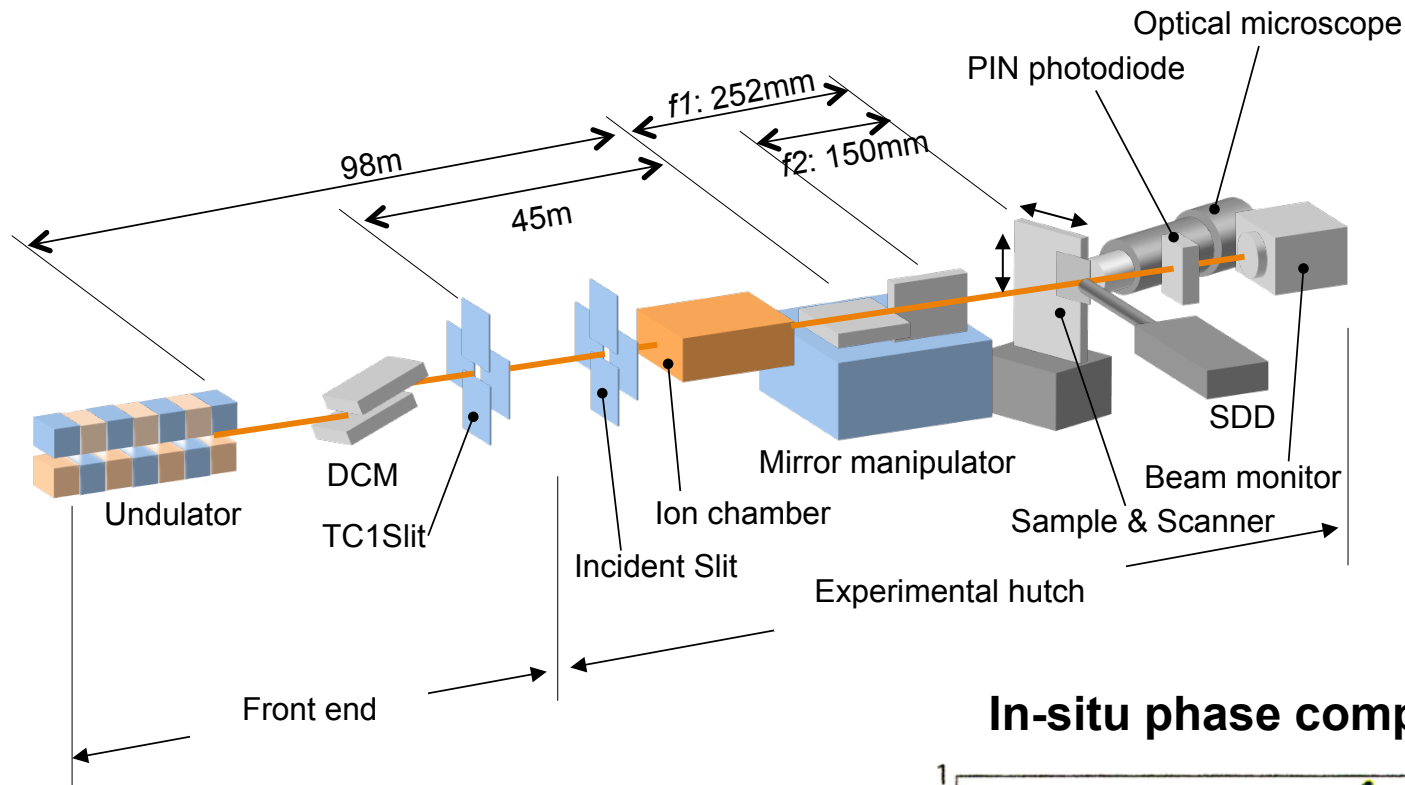
Fluorescent microscope image



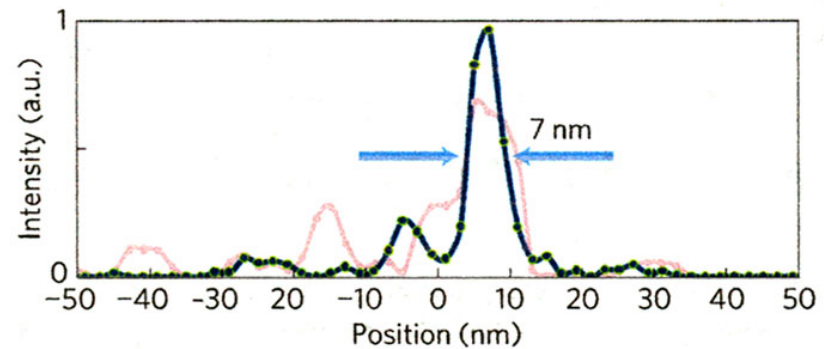
S. Matsuyama et al.,  
*X-Ray Spectrom.*(2010).

Courtesy of K. Yamauchi and  
H. Mimura, Osaka University.

# X-ray microprobe at SPring-8



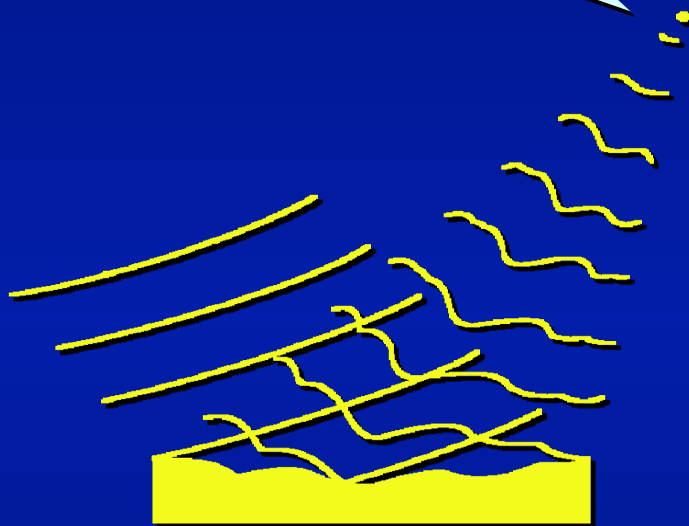
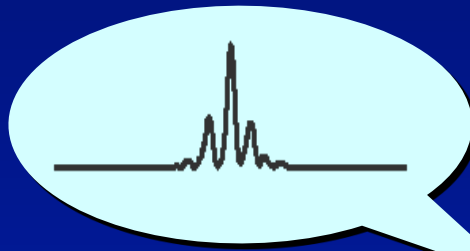
## In-situ phase compensation



Courtesy of K. Yamauchi and  
H. Mimura, Osaka University.

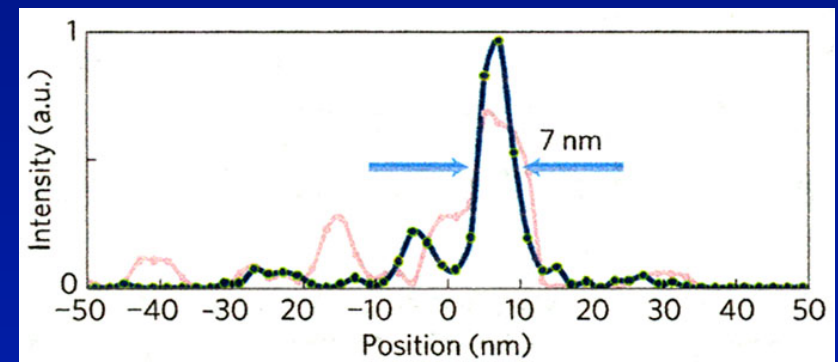
H. Mimura et al., *Nature Physics*, **6**, 122 (2009)



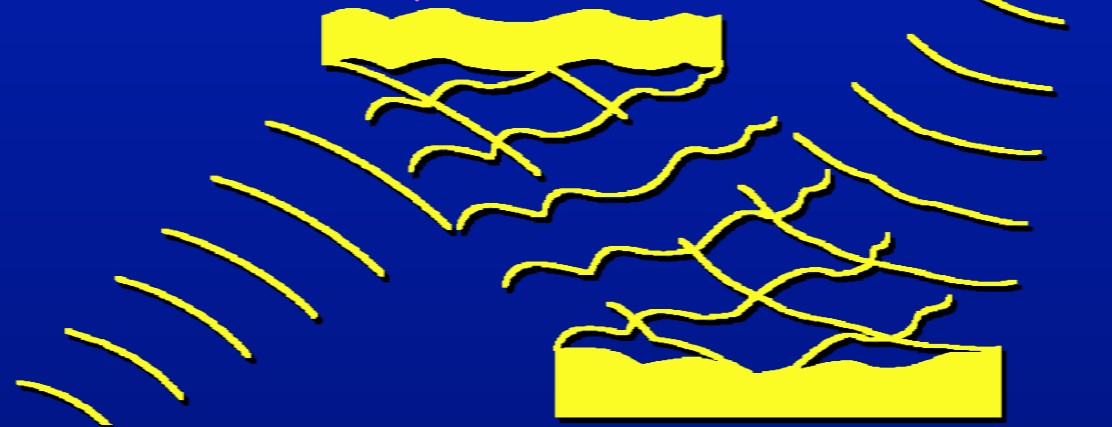


Focusing mirror with phase error

## *In-situ phase compensation*



## *Piezo-electric phase compensator*

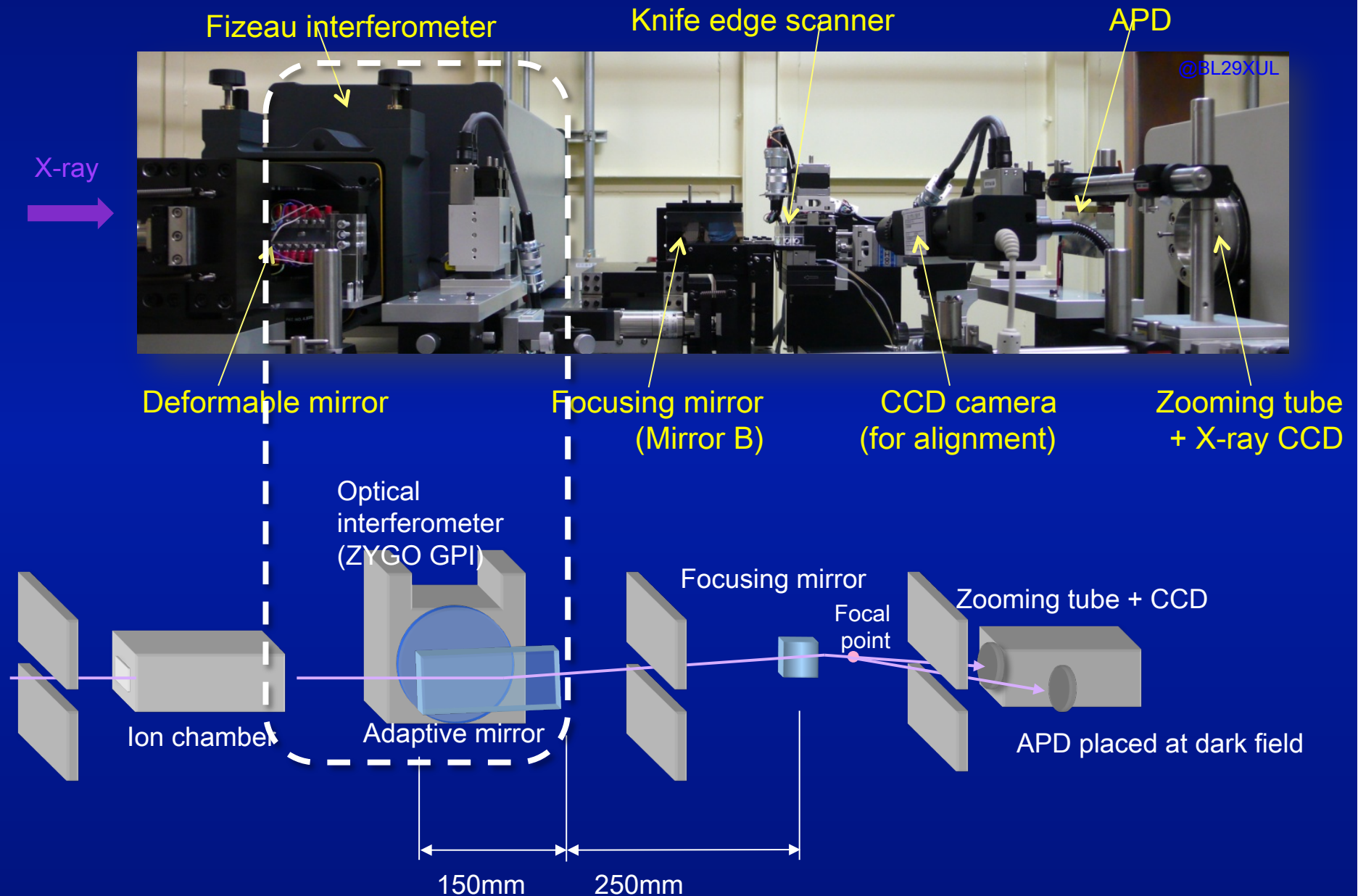


Focusing mirror with phase error

H. Mimura et al., *Nature Physics*, **6**, 122 (2009)

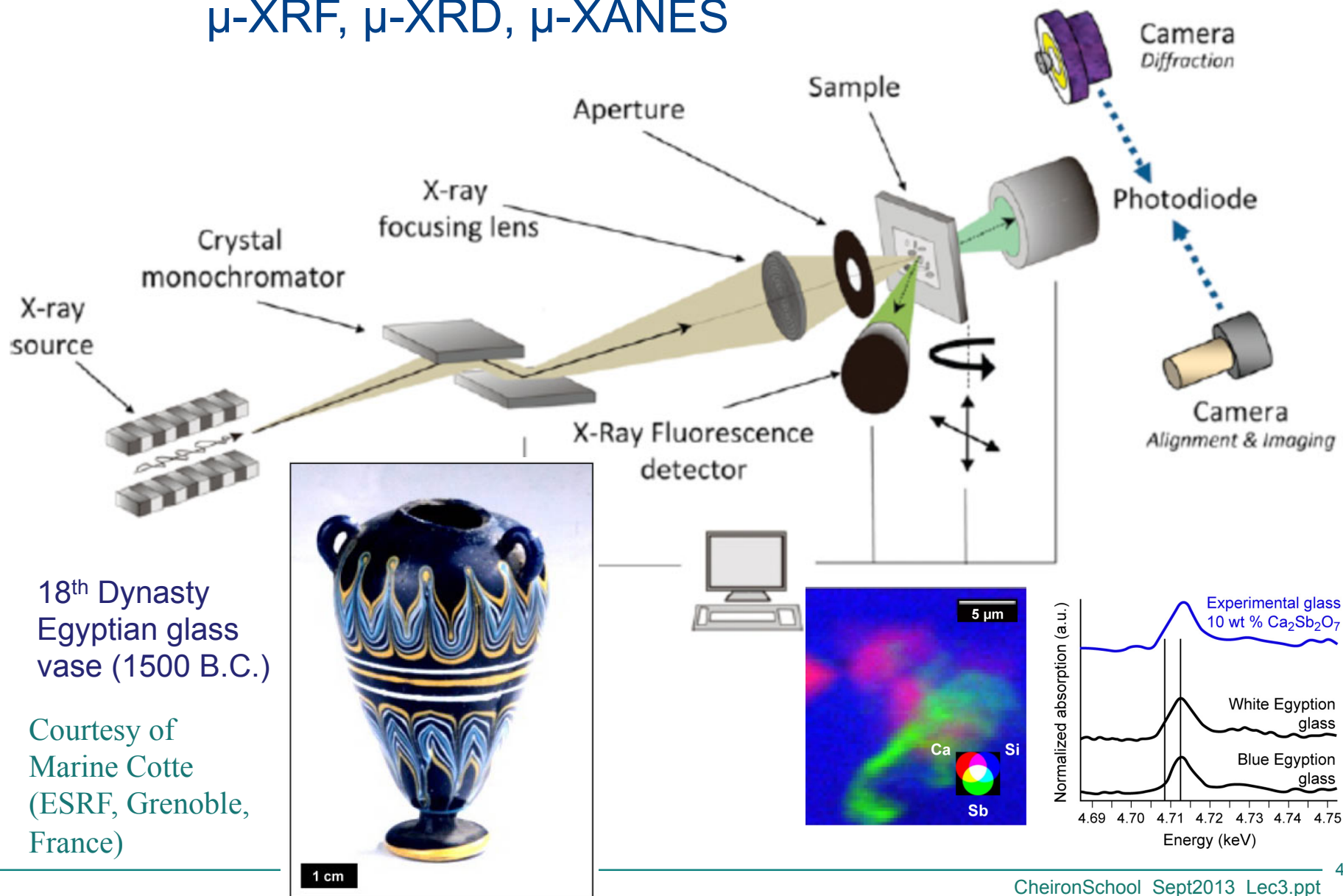
# Optical configuration for active phase compensation

41



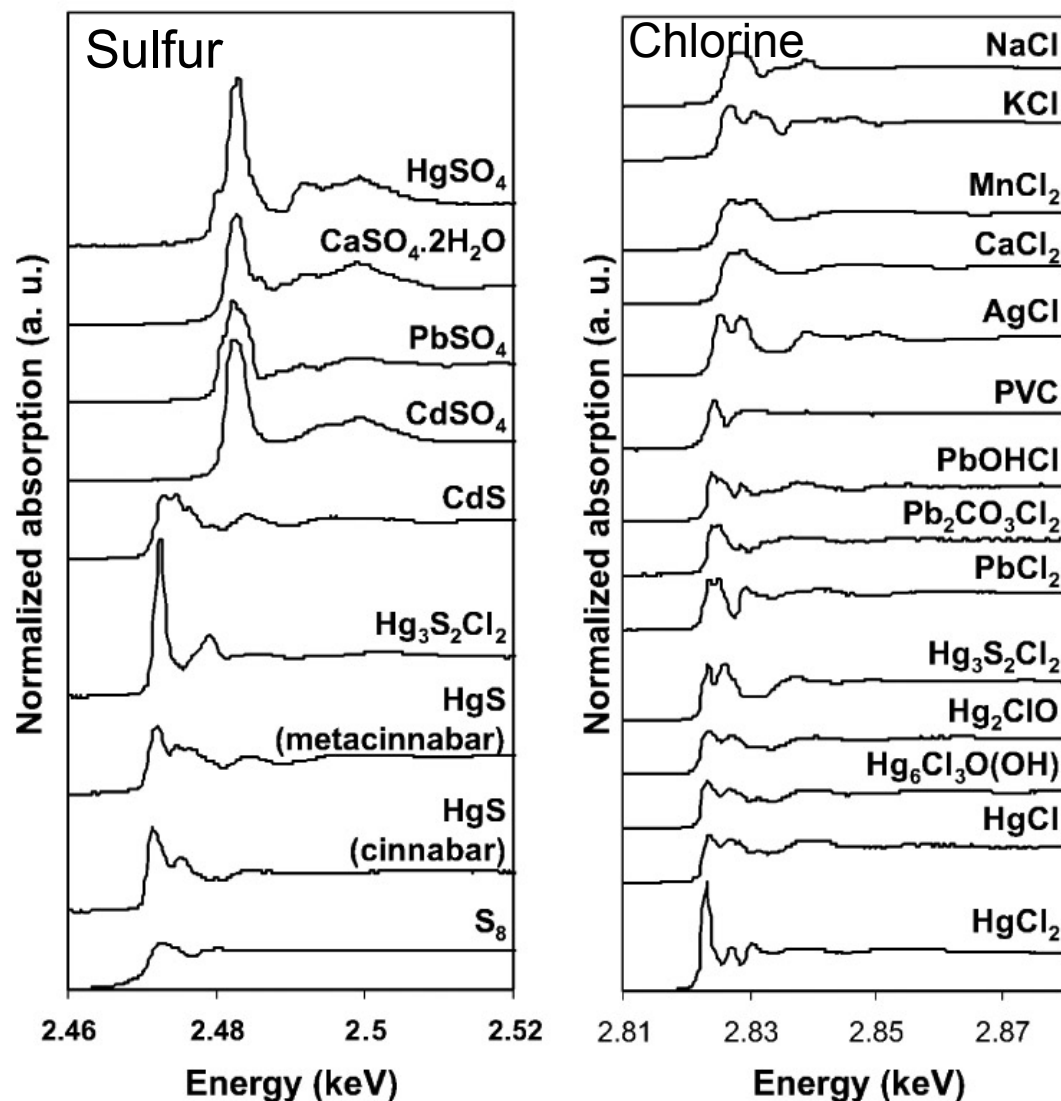
# Synchrotron-based art conservation at ESRF

$\mu$ -XRF,  $\mu$ -XRD,  $\mu$ -XANES





# Examples of $\mu$ -XANES K-edge spectra occurring in art materials

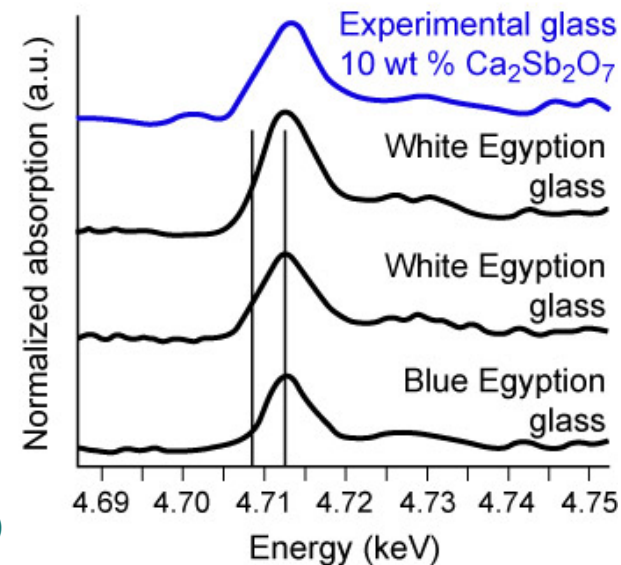
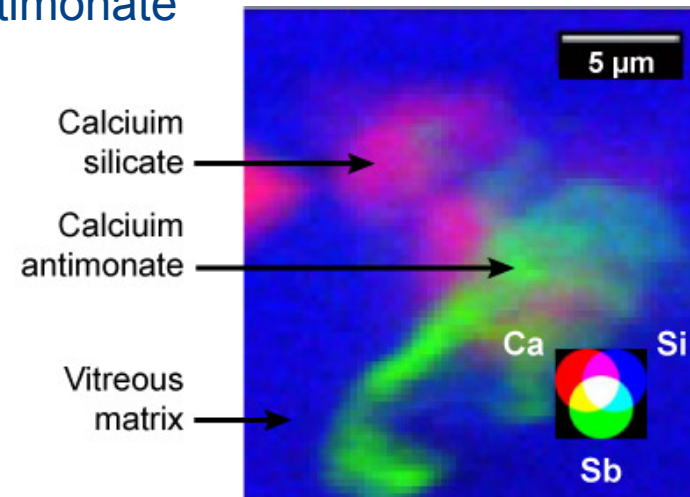


Courtesy of Marine Cotte (ESRF, Grenoble, France)

# 18<sup>th</sup> Dynasty Egyptian glass vase studied for an understanding of color and opaqueness in antiquity

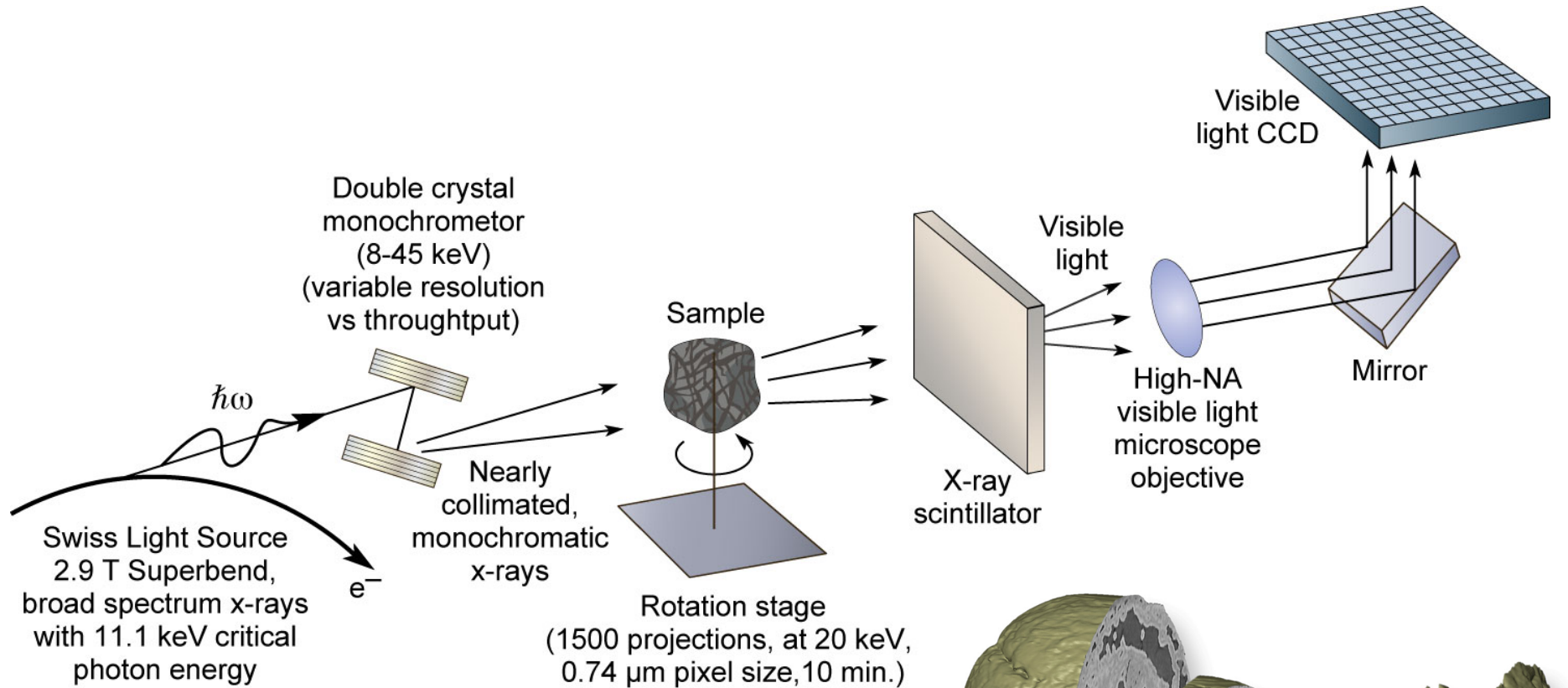


1<sup>st</sup> production of glass objects Egypt (1500 B.C.),  
opaque, colored, nanoscale calcium antimonate

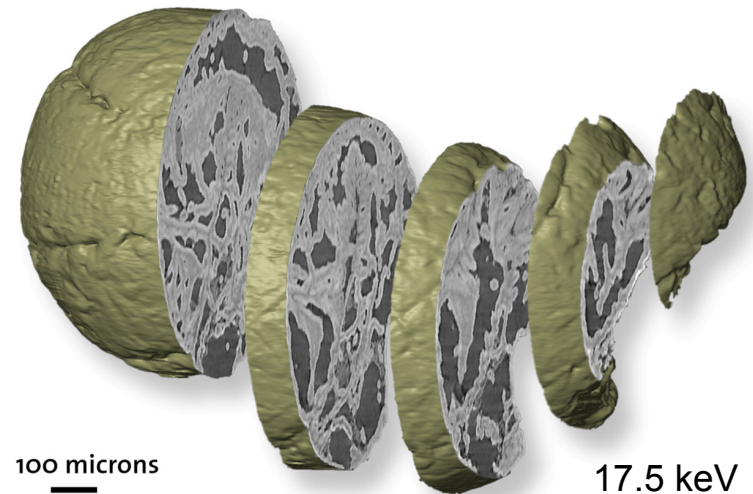


Courtesy of Marine Cotte (ESRF, Grenoble, France)

# Synchrotron radiation x-ray tomographic microscopy (SRXTM)



Tomographic reconstruction of a 500 million year old fossilized embryo from Southern China

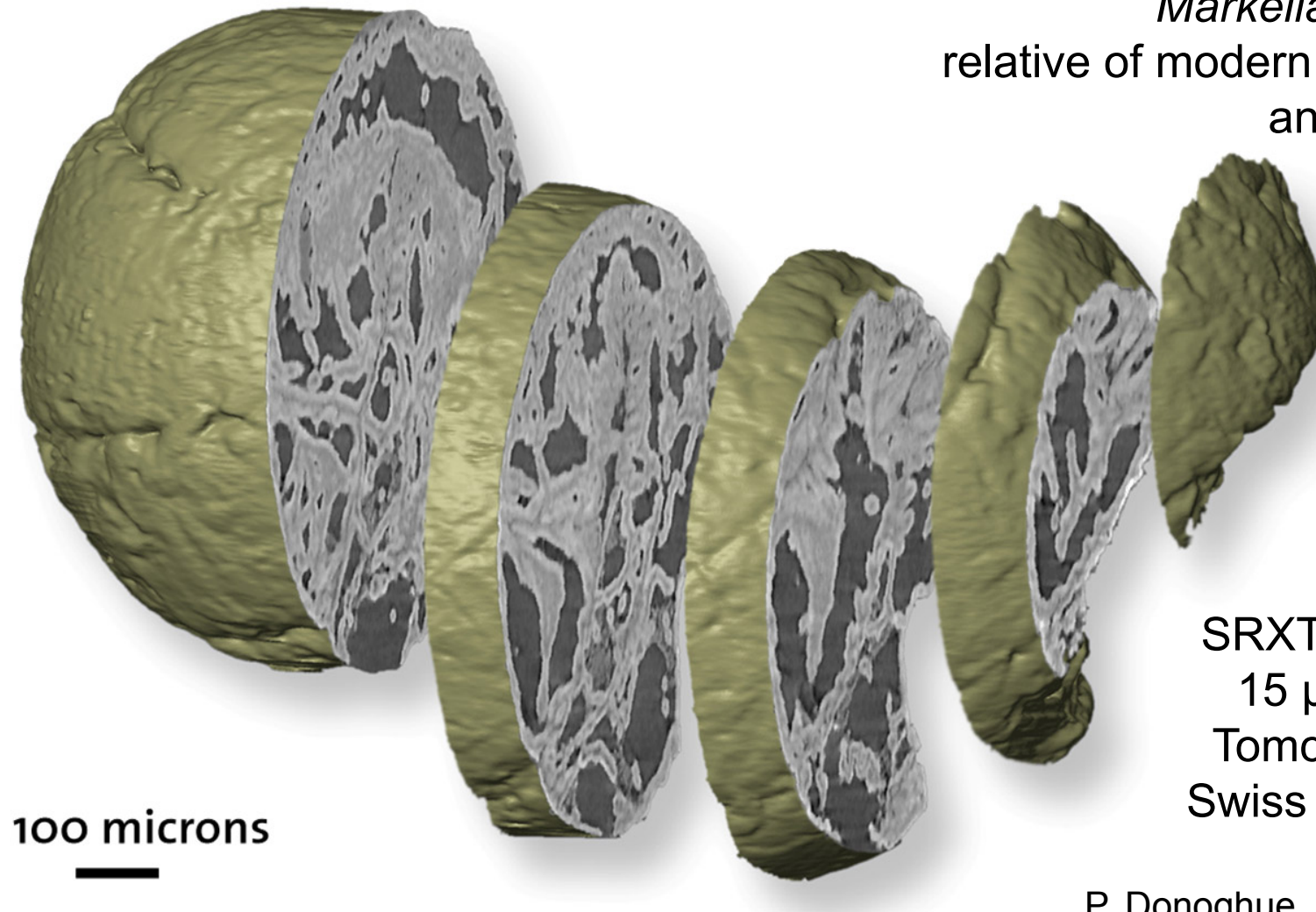


P. Donoghue, S. Bengtson, M. Stampanoni et al., *Nature* 442, (2006)



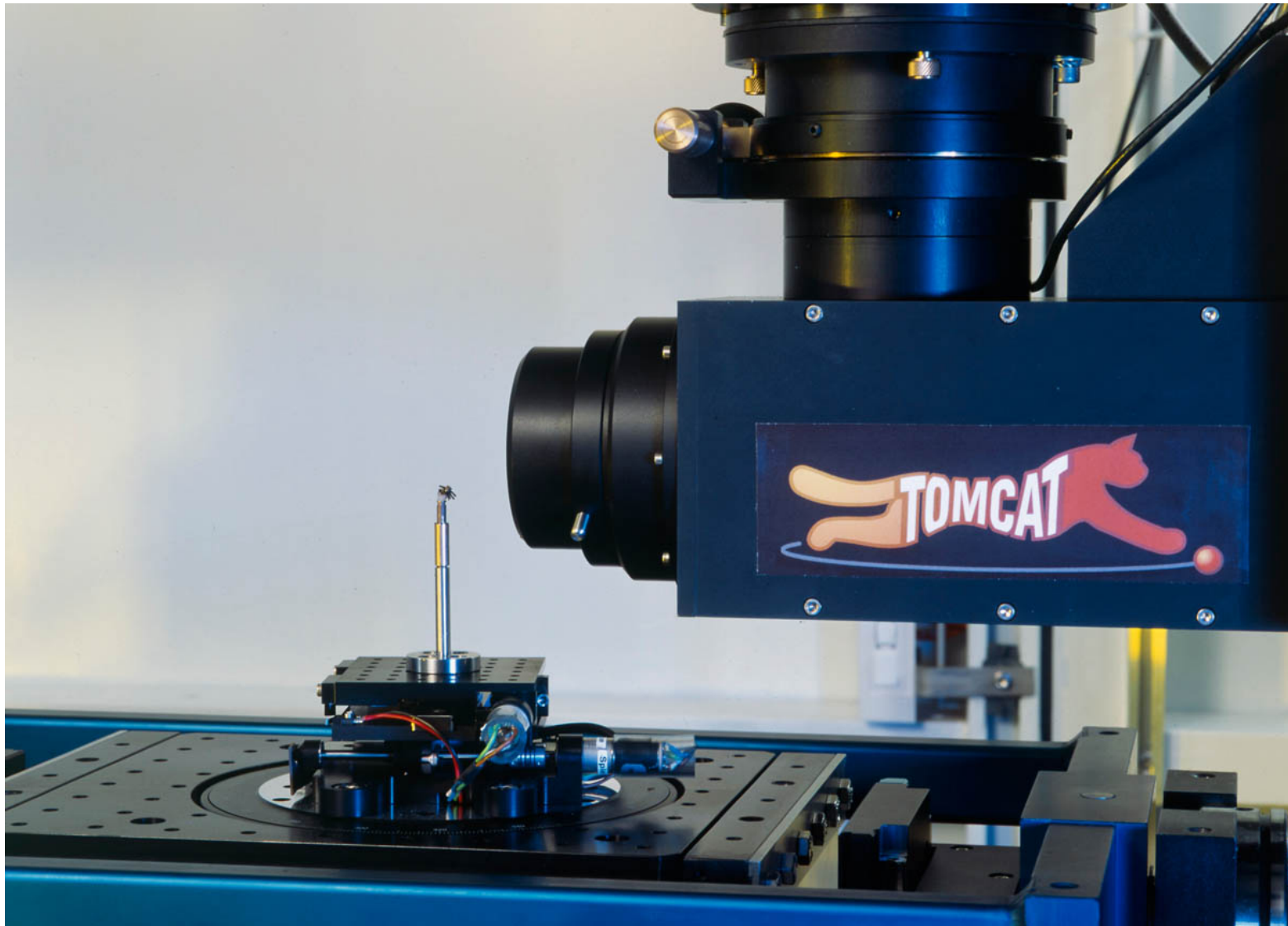
# Tomographic reconstruction of a 500 million year old fossilized embryo from Southern China

*Markelia hunanensis*  
relative of modern roundworms  
and arthropods

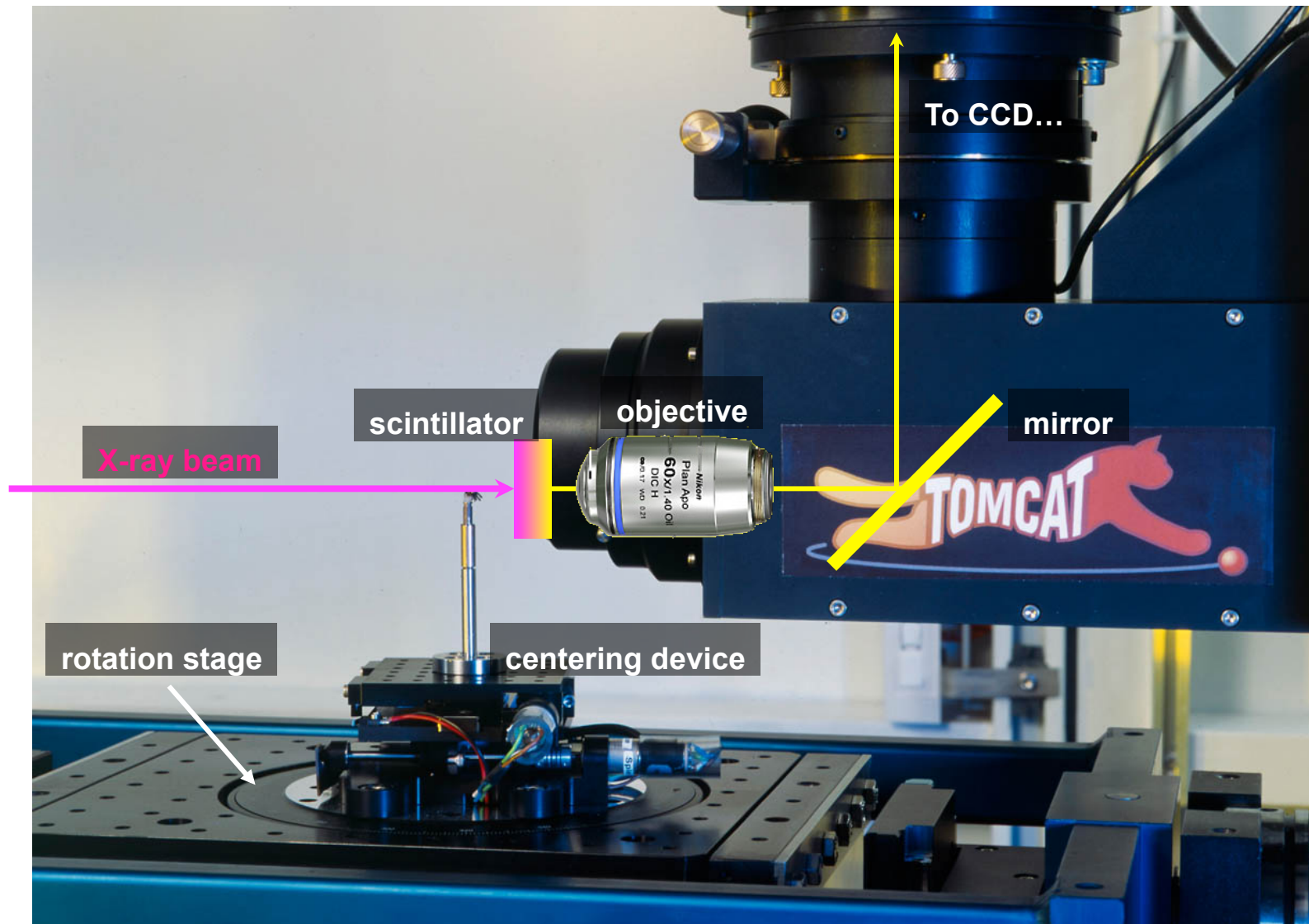


SRXTM, 17.5 keV,  
15  $\mu$ m resolution  
Tomcat Beamline,  
Swiss Light Source

P. Donoghue, S. Bengtson, M.  
Stampanoni et al., *Nature* 442, (2006)



# TOMCAT Microscope





## Hard x-ray 3D x-ray tomography: microvascular architecture of a mouse brain



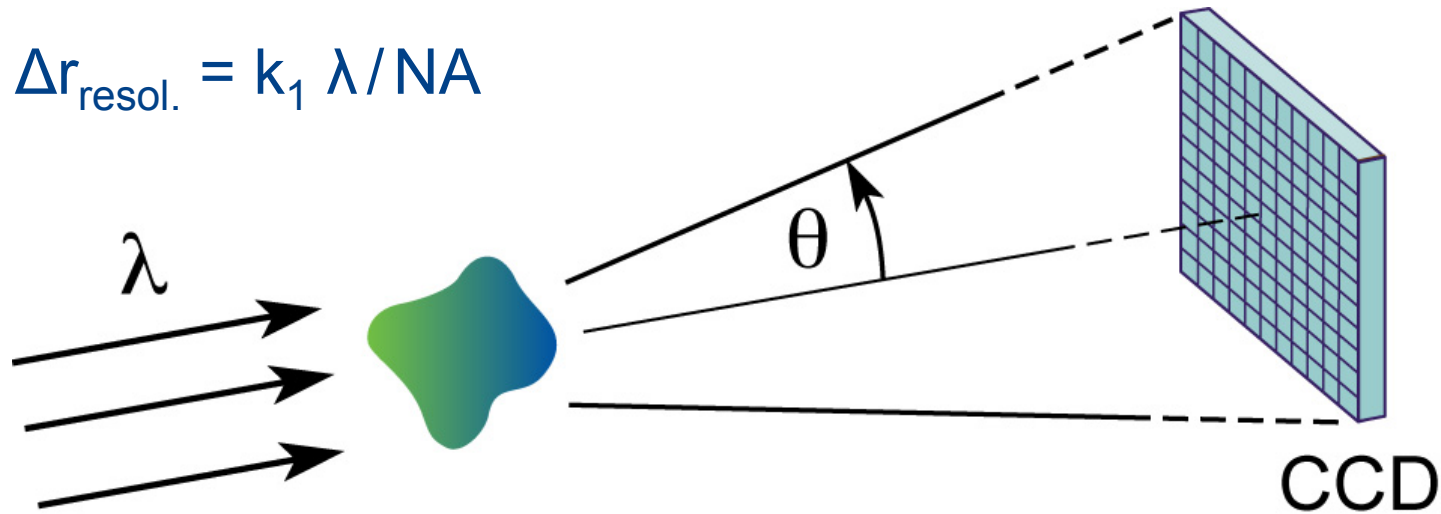
SRXTM, 25 keV,  
15  $\mu\text{m}$  resolution  
Tomcat Beamline,  
Swiss Light Source

M. Stampanoni,  
T. Krucker et al.,  
*Adv. Neur. Res.* (2008)



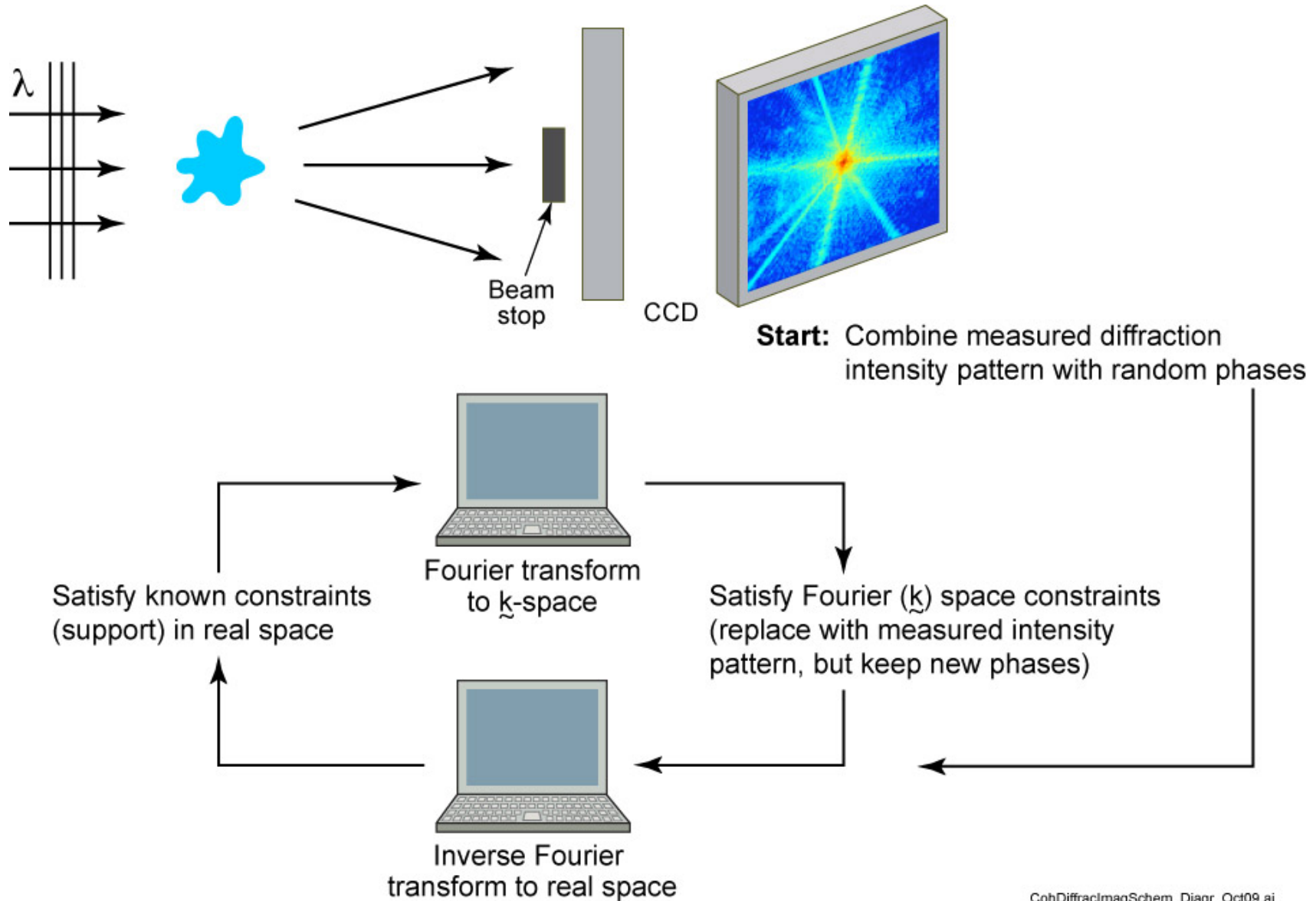
## A lens is not necessarily required

$$\Delta r_{\text{resol.}} = k_1 \lambda / \text{NA}$$



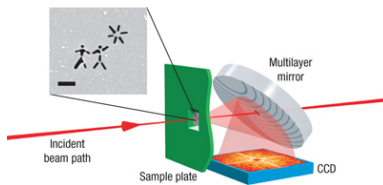
“Lensless” coherent diffraction imaging (CDI) is being aggressively pursued.

# Coherent diffractive imaging (CDI)



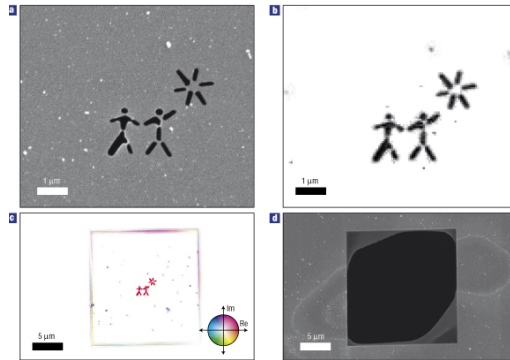
# Coherent diffractive imaging (CDI) examples

## Femtosecond diffractive imaging with a free electron laser



Flash FEL,  $\lambda = 32$  nm (39 eV)  
25 fsec,  $10^{12}$  photons/pulse  
62 nm resolution

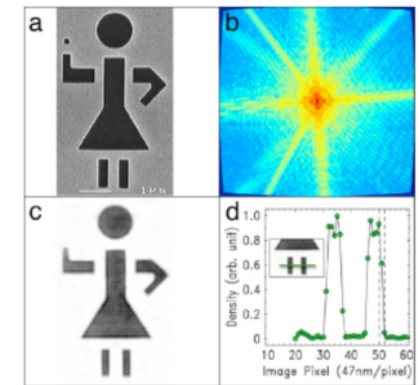
Chapman, et al. Nature Physics (2006)



## CDI with laboratory scale high harmonic generation (HHG)

HHG,  $n = 27$ ,  $\lambda = 29$  nm (43 eV)  
94 nm spatial resolution

Sandberg, et al. PNAS (2008)



## Synchrotron based CDI of 100 nm Au spheres

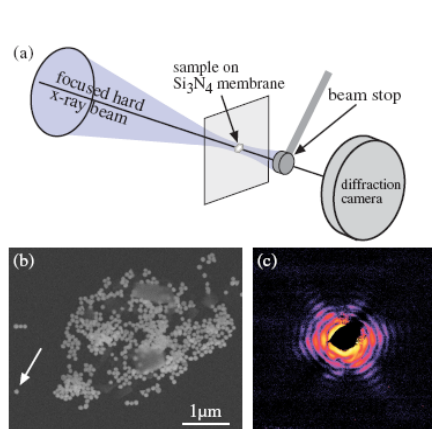


FIG. 1 (color online). (a) Schematic sketch of the coherent diffraction imaging setup with nanofocused illumination. (b) Scanning electron micrograph of gold particles (diameter  $\approx 100$  nm) deposited on a  $\text{Si}_3\text{N}_4$  membrane. (c) Diffraction pattern (logarithmic scale) recorded of the single gold particle pointed to by the arrow in (b) and illuminated by a hard x-ray beam with lateral dimensions of about  $100 \times 100$  nm $^2$ . The maximal momentum transfer, both in horizontal and vertical direction, is  $q = 1.65$  nm $^{-1}$ .

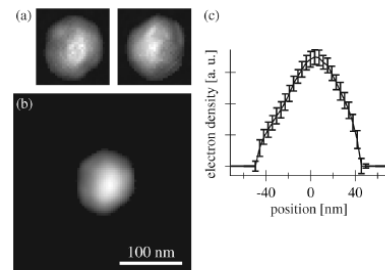


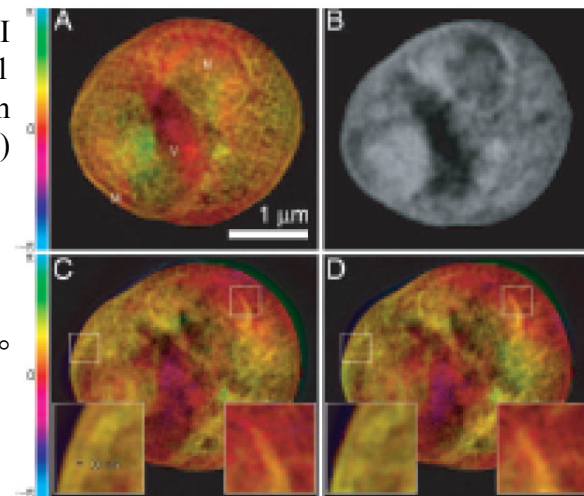
FIG. 2. (a) Two individual reconstructions of the gold particle using the HIO algorithm, a left- and a right-handed one. To obtain the average particle shape from a series of reconstructions with random initial phases, the right-handed reconstructions were inverted and averaged together with the left-handed ones. (b) Reconstructed projected electron density of the gold nanoparticle shown in Fig. 1(b) after averaging the series of reconstructions. (c) Horizontal section through the center of the particle shown in (b). The error bars indicate rms variations in the density for the series of independent reconstructions.

Synchrotron CDI of Au particles  
 $\lambda = 0.083$  nm (15 keV),  
5 nm “resolution”  
Schroer, et al. PRL (2008)

## Synchrotron based CDI of a freeze dried yeast cell

CDI  
ALS/9.0.1  
 $\lambda = 1.66$  nm  
(750 eV)

Tilted 3°

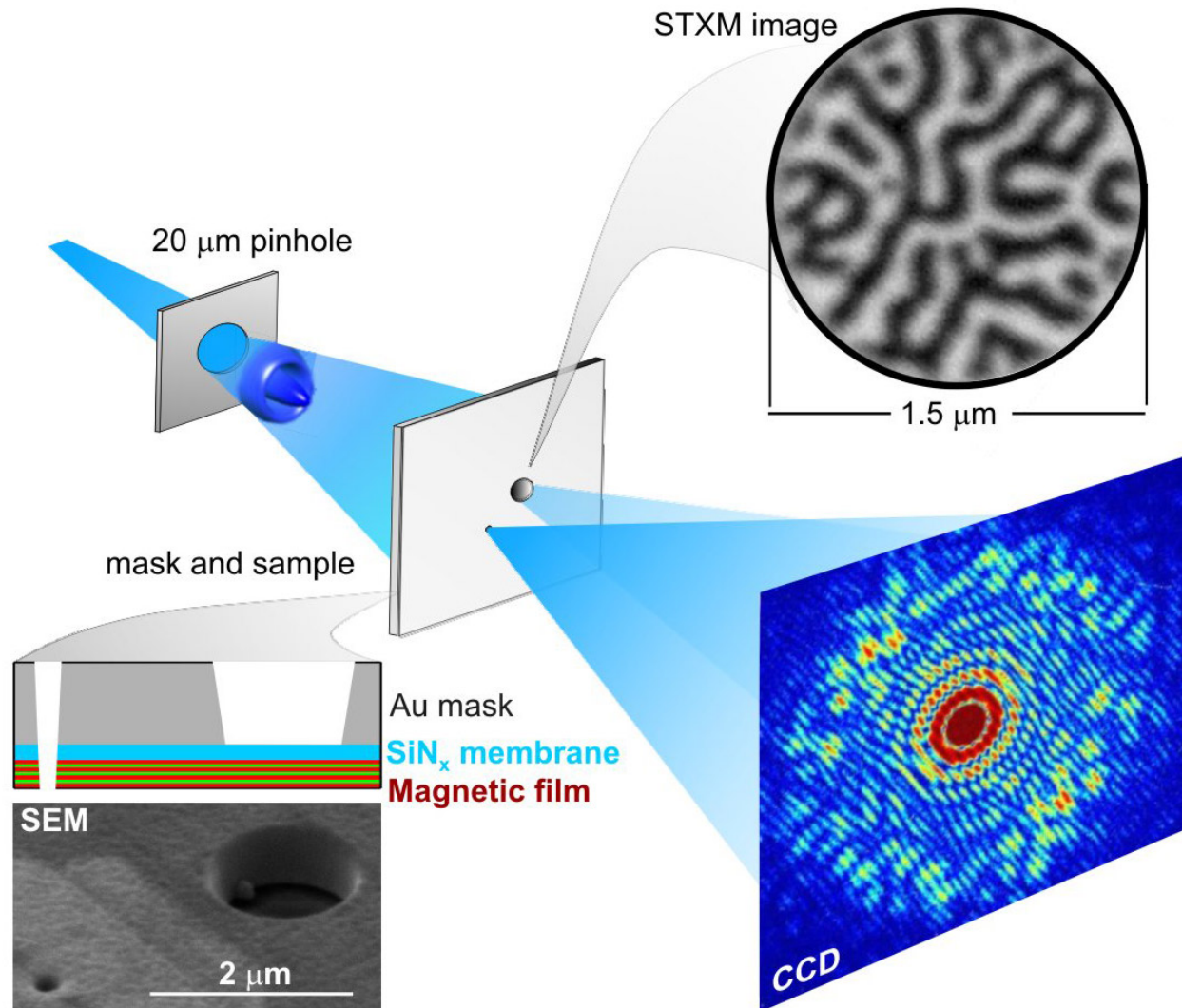


STXM  
NSLS/X1  
 $\lambda = 2.3$  nm  
(540 eV)  
42 nm  
resolution

Tilted 4°

Shapiro, et al. PRL (2005)

30 nm fine features

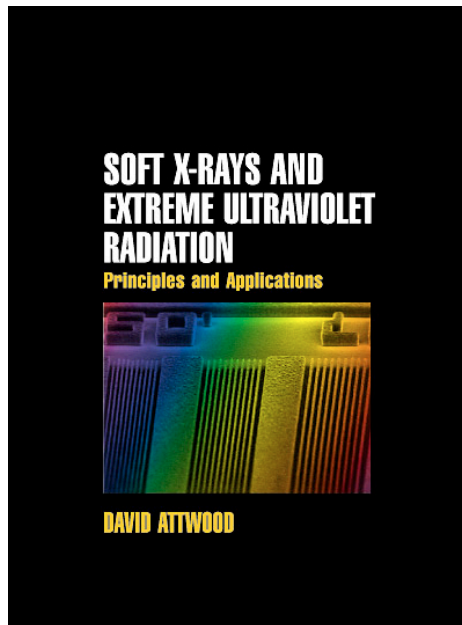


S. Eisebitt, J. Lüning, W.F. Schlotter, M. Lörger, O. Hellwig,  
W. Eberhardt & J. Stöhr / *Nature*, 16 Dec 2004

LenslessImagingF1.ai



# Lectures online at [www.youtube.com](http://www.youtube.com)



Amazon.com



**UC Berkeley**

[www.coe.berkeley.edu/AST/sxreuv](http://www.coe.berkeley.edu/AST/sxreuv)

[www.coe.berkeley.edu/AST/srms](http://www.coe.berkeley.edu/AST/srms)

[www.coe.berkeley.edu/AST/sxr2009](http://www.coe.berkeley.edu/AST/sxr2009)